

IN-71

40039

P.66

NASA Contractor Report 187558

Analysis of Interior Noise Ground and Flight Test Data for Advanced Turboprop Aircraft Applications

M.A. Simpson and B.N. Tran

**DOUGLAS AIRCRAFT COMPANY
MCDONNELL DOUGLAS CORPORATION
LONG BEACH, CA 90846**

**CONTRACT NAS1-18037
AUGUST 1991**



National Aeronautics and
Space Administration

Langley Research Center
Hampton, Virginia 23665-5225

(NASA-CR-187558) ANALYSIS OF INTERIOR NOISE
GROUND AND FLIGHT TEST DATA FOR ADVANCED
TURBOPROP AIRCRAFT APPLICATIONS Final Report
(Douglas Aircraft Co.) 66 p CSCL 20A

N91-31927

63/71 Unclas
0040039

•
•
•
•

NASA Contractor Report 187558

**Analysis of Interior Noise
Ground and Flight Test Data
for Advanced Turboprop
Aircraft Applications**

M.A. Simpson and B.N. Tran

**DOUGLAS AIRCRAFT COMPANY
MCDONNELL DOUGLAS CORPORATION
LONG BEACH, CA 90846**

**CONTRACT NAS1-18037
AUGUST 1991**



National Aeronautics and
Space Administration

Langley Research Center
Hampton, Virginia 23665-5225

Preface

This report was prepared by McDonnell Douglas Corporation under Task Assignment 8 of Contract NAS1-18037 with NASA Langley Research Center. The NASA technical monitor was Dr. Kevin P. Shepherd.

Several individuals at Douglas Aircraft Company made major contributions to this study. The ground tests described in this report were conducted by Don Daulton, Jim Phillips, and Dick Gordon, under the direction of Dr. Mark Lang. Mike Sundquist and Brian Hoare were responsible for data processing. Dr. Gopal Mathur and Dr. Mahendra Joshi reviewed the analyses and this report, and made many useful recommendations.

Contents

1	Introduction	1
2	Description of the Ground Tests	3
2.1	Fuselage Configurations	3
2.2	Noise and Vibration Sources	4
2.3	Test Points	5
2.4	Measurement and Processing Instrumentation	6
3	Ground Test Results	17
3.1	Interior Noise Levels	17
3.1.1	Speaker Excitation	17
3.1.2	Shaker Excitation	18
3.1.3	Speaker Plus Shaker Excitation	19
3.1.4	Speaker Array Excitation	19
3.2	Acceleration Levels	20
3.2.1	Speaker Excitation	20
3.2.2	Shaker Excitation	20
3.2.3	Speaker Plus Shaker Excitation	20
3.3	Sound Intensity Survey Results	21
4	Comparison of Ground and Flight Test Results	45
4.1	Identification of Major Transmission Paths	45
4.1.1	Ground Test Analysis of Transmission Paths	45
4.1.2	Comparison With Flight Test Analysis	47
4.2	Cabin Noise Levels	47
4.3	Evaluation of Treatment Effectiveness	49

5 Summary and Conclusions

55

6 References

58

List of Tables

1. Excitation Levels for Selected Tests	8
2. Comparison of Broadband Cabin Noise Levels Measured During Ground and Demonstrator Flight Tests	49
3. Noise Level Reduction Between Baseline and Quiet Cabin Configurations	51

List of Figures

1. The DC-9 Fuselage Test Section, Showing Frame and Longeron Numbering	9
2. Noise and Vibration Source Configurations for Ground Tests	10
3. Comparison of the Exterior Acoustic Loads Distribution for BPF(8), Demo Vs Ground Simulation	11
4. Exterior Microphone Locations	12
5. Cabin and Aft Section Microphone Locations	13
6. Location of Pylon and Fuselage Accelerometers	14
7. Frame and Aft Bulkhead Accelerometer Locations	14
8. Sound Intensity Survey Areas	15
9. Location of Sound Intensity Survey Grids	16
10. Normalized Cabin Noise Levels due to Speaker Excitation, Baseline Configuration	22
11. Normalized Cabin Noise Levels due to Shaker Excitation, Quiet Cabin Configuration	23
12. Variation of Maximum Cabin Noise Levels due to Speaker Excitation with Rotor Speed, Quiet Cabin Configuration	24
13. Effect of Pressurization on Cabin Noise Levels due to Speaker Excitation, Quiet Cabin Configuration	25
14. Comparison of Cabin Noise Levels due to Tonal and Broadband Excitation, Quiet Cabin Configuration	26
15. Normalized Cabin Noise Levels due to Shaker Excitation, Baseline Configuration	27
16. Normalized Cabin Noise Levels due to Shaker Excitation, Quiet Cabin Configuration	28
17. Variation of Maximum Cabin Noise Levels due to Shaker Excitation with Rotor Speed, Quiet Cabin Configuration	29
18. Effect of Pressurization on Cabin Noise Levels due to Shaker Excitation, Quiet Cabin Configuration	30
19. Comparison of Cabin Noise Levels due to Shaker Tonal and Broadband Excitation, Quiet Cabin Configuration	31

20. Cabin Noise Levels due to Combined Speaker and Shaker Excitation, Quiet Cabin Configuration	32
21. Effect of Variation in Relative Phase Between Speaker and Shaker Excitation on Cabin Noise Levels due to Combined Excitation, Quiet Cabin Configuration ..	33
22. Noise Spectra at Seat 5, Row 5 due to Loudspeaker Array Excitation, Baseline Configuration	34
23. Noise Spectra at Seat 5, Row 5 due to Loudspeaker Array Excitation, Quiet Cabin Configuration	35
24. Effect of Pressurization on Noise Spectra at Seat 5, Row 5 due to Loudspeaker Array Excitation, Quiet Cabin Configuration	36
25. Normalized Frame 758 Accelerometer Levels due to Speaker Excitation, Baseline Configuration	37
26. Normalized Frame 758 Accelerometer Levels due to Speaker Excitation, Quiet Cabin Configuration	38
27. Normalized Frame 758 Accelerometer Levels due to Shaker Excitation, Baseline Configuration	39
28. Normalized Frame 758 Accelerometer Levels due to Shaker Excitation, Quiet Cabin Configuration	40
29. Frame 758 Accelerometer Levels due to Combined Speaker and Shaker Excitation, Quiet Cabin Configuration	41
30. Sound Power Levels due to Speaker Excitation in the 160, 200, 315 Hz One-Third Octave Bands, Quiet Cabin Configuration	42
31. Sound Power Levels due to Shaker Excitation in the 160, 200, 315 Hz One-Third Octave Bands, Quiet Cabin Configuration	43
32. Sound Power Levels due to Speaker Array Excitation in the One-Third Octave Bands from 100-500 Hz, Quiet Cabin Configuration	44
33. Comparison of Cabin Noise Levels Scaled from Ground Test Measurements with Flight Test Data, Quiet Cabin Configuration	52
34. Comparison of Maximum Cabin Noise Levels Measured During Demonstrator and Ground Tests for Varying Rotor Speed, Quiet Cabin Configuration	53
35. Exterior and Interior Spectra due to Speaker Array Excitation Measured During Ground Tests, Quiet Cabin Configuration	54

1 Introduction

This report is the fourth in a series of NASA-sponsored reports which deal with the control of interior noise levels on advanced turboprop aircraft. The first report (Reference [1]) describes the results of ground tests to evaluate the effectiveness of a variety of candidate noise control treatments. Measurements were conducted on a DC-9 aircraft test section using laboratory sources to simulate the acoustic and vibratory loads of advanced turboprop engines. The second report (Reference [2]) documents noise and vibration levels measured during flight tests of a Demonstrator aircraft, which was an MD-80 aircraft equipped with one prototype advanced turboprop engine (designated as an Ultra High Bypass or UHB engine), and containing several of the treatments evaluated during the prior ground tests. The third report (Reference [3]) addresses the response of the DC-9 fuselage section during ground testing under various types of acoustic and vibration excitation, including the shell and cavity modal properties and structural-acoustic coupling characteristics.

Over the past four years, McDonnell Douglas Corporation (MDC) has conducted a significant amount of ground and flight testing to design and evaluate effective interior noise control treatments for advanced turboprop aircraft. It may be expected that flight testing provides the most accurate approach to preliminary identification and diagnosis of interior noise problems and to subsequent evaluation of treatment effectiveness for new or derivative aircraft. Unfortunately, when such aircraft are in the development stage, flight testing is usually limited (due to cost and time constraints) or non-existent (if the new aircraft is not yet fabricated or flight-worthy). Thus the acoustics design engineer typically relies heavily, if not exclusively, on ground test data. The applicability of such data for noise control development must consider the differences in noise and vibration characteristics between the lab sources and the actual engine, differences in the propagation characteristics and the modal response between the ground test article and the actual aircraft, flight effects, etc. The availability of the DC-9 ground test facility and the Demonstrator flight test data at MDC has provided an opportunity to assess these effects on interior noise design and evaluation.

The primary objective of the work described in this report, then, is to study ground test and analysis techniques for evaluating the effectiveness of interior noise control treatments for advanced turboprop aircraft. A secondary objective is to study the sensitivity of the ground test results to changes in various test conditions. To meet these objectives ground tests were conducted using the DC-9 fuselage section and simulated advanced turboprop sources, and the ground measurement results were compared with the measurement results obtained during the earlier Demonstrator flight tests (Reference [2]). Selected ground test conditions were also parametrically varied to examine sensitivity effects.

The next section of this report documents the ground tests. Section 3 provides detailed ground test results for two noise control treatment configurations, and for the various sensitivity tests. In Section 4 the ground test results are compared with the Demonstrator flight test results, in terms of transmission path identification, cabin noise levels, and treatment effectiveness. Major conclusions are summarized in the final text section.

2 Description of the Ground Tests

The ground tests were conducted between August and November 1990 in the Fuselage Acoustics Research Facility (FARF) at Douglas Aircraft Company (DAC). This facility consists of the aft section of a DC-9 aircraft fuselage in a large anechoic chamber, noise and vibration sources to simulate a variety of excitations including advanced turboprop engine noise and vibration, and a multi-channel digital data acquisition and processing system. Figure 1 shows the fuselage test section, with the frame station and longeron numbering system. Additional details about FARF and its components may be found in Reference [1].

2.1 Fuselage Configurations

The ground tests were conducted in two phases, corresponding to two fuselage treatment configurations. These configurations were selected to represent the Baseline and Quiet Cabin Configurations used during the Demonstrator flight test program (see Reference [2] for a detailed description of the Demonstrator configurations). The Baseline Configuration on the Demonstrator consisted of additional frames in the aft cabin (including a torque box frame), damping material on the new and existing frames, a double wall attached to the pressure bulkhead, sonic fatigue damping material applied to the skin in the aft section and cabin area, acoustic damping material applied to the skin in the cabin and cargo compartments, floor isolation, and absorption blankets in the aft section. The cabin was unfurnished, but included two layers of sidewall thermal insulation. For the ground tests in FARF, the Baseline Configuration was identical with the following exceptions: (1) the torque box frame was disabled but still installed on the fuselage structure, (2) no floor isolation, and (3) uniform application of the sonic fatigue damping material around the entire DC-9 fuselage circumference (on the Demonstrator this material is installed only on the UHB engine side).

The Quiet Cabin Configuration on the Demonstrator included all the Baseline treatments plus damping on the torque box, engine dynamic absorbers, damped trim panels, and complete cabin furnishings (carpeting on the floor and engine pylon bulkhead walls, seats, baggage racks, ceiling panels, and a coat closet on the left side of the cabin between the last seat row and the lavatory). For the ground tests in FARF, the Quiet Cabin Configuration was identical with the following exceptions: (1) the torque box was still disabled, and (2) there were no engine dynamic absorbers (there were no engines!).

The ground and flight test programs also included sound intensity surveys in the cabin for dominant source and path identification. These surveys were made in the Quiet Cabin Configuration with some modifications needed to ensure good quality data and useful diagnostic information. These modifications included removal of the

double wall over the pressure bulkhead door (but not over the remaining sections of the pressure bulkhead behind the two lavatories), removal of the carpeting on the floor and engine pylon bulkhead walls, removal of the seats, removal of the coat closet, and the use of Sonex foam at various locations in the cabin to ensure an adequate acoustic environment for the survey.

To simulate in-flight conditions the fuselage was pressurized to a pressure differential of 5 psi during all ground tests except pressurization sensitivity tests in which the pressure differential was varied. Also, since the sound intensity survey required an engineer to be in the cabin, the fuselage was not pressurized for this test.

2.2 Noise and Vibration Sources

The noise spectrum in the aft cabin of the Demonstrator is characterized by several distinct tones superimposed on a broadband background. These tones occur at the blade passage frequencies associated with the two propeller rotors of the UHB engine and at the shaft rotational frequencies of the engines, plus the harmonics of these frequencies. The primary tones in the interior spectrum due to the UHB engine were found to occur at the blade passage frequency (BPF) and its first harmonic (2BPF), and at the UHB N1 shaft rotational frequency (designated UN1). The BPF and 2BPF tones could propagate into the cabin through airborne and/or structureborne paths, while the UN1 tone could propagate through only a structureborne path. The broadband background noise results from the turbulent boundary layer noise transmitted through the aircraft sidewall into the cabin.

Three different sources were used in the ground tests to simulate the acoustic and vibration excitations experienced by the Demonstrator. The first source was a single loudspeaker located outside the aft fuselage on the left side at station 908, approximately 4 feet from the fuselage (see Figure 2). This speaker was used as an airborne source of UHB tones, that is, as a source of the acoustic loads impinging on the aft fuselage at the blade passage frequencies. Since Demonstrator flight tests were conducted with first an 8x8 UHB engine and then a 10x8 UHB engine (the number of blades in the forward fan rotor x the number of blades in the aft fan rotor), the tones generated through this speaker included those at the blade passage frequencies for both the 8-bladed and 10-bladed rotors (designated BPF(8) and BPF(10), respectively). The 2BPF(8) tone was also reproduced through the speaker. For a typical engine speed of 1260 rpm, the frequencies corresponding to BPF(8), BPF(10), and 2BPF(8) are 168, 210, and 336 Hz, respectively.

Measurements on the exterior of the Demonstrator showed that the noise levels on the aft fuselage surface in the plane of the propeller were very high, but diminished

rapidly at locations forward of the propeller planes. To simulate this directivity, a barrier was erected around the speaker to reduce levels forward of the propeller plane (see Figure 2). Figure 3 compares the directivity of the BPF(8) tone measured on the Demonstrator with the directivity measured during the ground tests from the single speaker with barrier.

The second source was a shaker attached to the forward engine mount on the left engine pylon, at an angle of 45 degrees to the vertical (see Figure 2). This shaker was used as a source of structureborne tones, such as might be generated by engine imbalances. In addition to tones at BPF(8), BPF(10), and 2BPF(8), the shaker produced a fourth tone at the UN1 frequency (185 Hz).

The third source consisted of two arrays of loudspeakers, each in a 5 by 5 configuration, located on either side of the fuselage (see Figure 2) about 5 feet from the fuselage surface. Broadband noise was played through these speakers to simulate exterior turbulent boundary layer noise. The levels of the individual speakers in the arrays were adjusted so that the spectra on the fuselage surface were nearly flat from 100 to 1000 Hz, as measured at several locations between stations 642 and 718.

2.3 Test Points

For each of the two test phases (Baseline Configuration and Quiet Cabin Configuration), noise and vibration data were collected for excitation of the fuselage by each of the three sources described above, singly and in combination. Following is a summary of the excitations used:

- Speaker tones at nine engine speeds (1170 to 1290 rpm, at 15 rpm increments)
- Speaker tones at multiple excitation levels (one engine speed, 1260 rpm)
- Speaker tones at multiple cabin pressurization levels (one engine speed, 1260 rpm)
- Shaker tones at nine engine speeds (1170 to 1290 rpm, at 15 rpm increments)
- Shaker tones at multiple excitation levels (one engine speed, 1260 rpm)
- Shaker tones at multiple cabin pressurization levels (one engine speed, 1260 rpm)
- Speaker plus shaker tones at multiple shaker excitation levels (one engine speed, 1260 rpm)
- Speaker plus shaker tones at multiple relative phases (one engine speed, 1260 rpm)

- Speaker array broadband noise at multiple excitation levels
- Speaker array broadband noise at multiple cabin pressurization levels
- Speaker array broadband noise plus speaker tones plus shaker tones (one engine speed, 1260 rpm)
- Speaker broadband noise
- Shaker broadband vibration

The sound intensity survey conducted during the Quiet Cabin Configuration phase consisted of three separate excitations:

- Speaker tones (one excitation level, one engine speed, 1260 rpm)
- Shaker tones (one excitation level, one engine speed, 1260 rpm)
- Speaker array broadband noise (one excitation level)

Within each test phase, the tests involving speaker tones alone were designated as “A” tests, shaker tests alone were designated as “B” tests, shaker plus speaker tests were designated as “C” tests, and all speaker array tests were designated as “D” tests. Table 1 below lists various tests conducted in each phase and the relative source excitation level used in each for test. For the tests with speaker or speaker array sources, the levels in the table refer to the sound pressure level at the appropriate reference microphone. For the tests with the shaker source, the levels in the table refer to the acceleration at the appropriate accelerometer (see discussion in Section 3).

2.4 Measurement and Processing Instrumentation

During the ground tests, data were acquired by exterior (fuselage surface) and interior microphones and pylon, frame, and pressure bulkhead accelerometers.

Exterior microphones were mounted on the left side of the fuselage 0.5 inch from the fuselage surface at the locations shown in Figure 4; the reference microphones for the aft speaker and the speaker arrays are indicated on the figure. Interior microphones were positioned in the aft cabin at 17 locations representing passenger seated and standing head heights as shown in Figure 5, and at the two locations in the unpressurized section also shown in the figure. Note that exterior and interior microphone locations in FARF are comparable to locations used during the Demonstrator flight tests. Each

microphone measurement system consisted of a B&K 4134 1/2 inch microphone with a Genrad 1560-P42 preamplifier and Pacific and Ithaco amplifiers.

Accelerometers were mounted on the left side pylon and aft fuselage as shown in Figure 6, and at several locations on frame 758 and on the pressure bulkhead as shown in Figure 7. Each accelerometer measurement system consisted of an Endevco 2250A-10 accelerometer with an Endevco signal conditioner and Ithaco amplifier.

A force gauge was installed between the connecting rod (stinger) of the shaker and the fuselage. This transducer was used as a reference for the shaker input force to the structure. The force measurement system consisted of a B&K 8500 force gauge with B&K 1050 vibration exciter and Ithaco amplifier.

The microphone channels were calibrated periodically with a B&K 4220 piston-phone, which produces a constant 250 Hz signal at 124 dB. The accelerometer channels were similarly calibrated with a B&K 4294 calibrator exciter which produces a constant 159 Hz signal at 1 g (rms). The various amplifiers were set to provide a 1 volt input to the tape recorder corresponding to either 124 dB or 1 g, depending on transducer type. This same 1 volt signal level was then used as a surrogate calibration signal on subsequent data tapes.

Measured data were recorded on a Honeywell model 101 FM tape recorder. Annotation information and a time code were recorded on two additional recorder channels. The data tapes were then processed on a digital data acquisition and processing system consisting of a digitizer coupled to a DEC microVAX II computer. The system is designed to permit rapid calculation and display of a variety of time-series functions from which frequency domain data can subsequently be obtained. The sampling duration for each measurement in this test program was 1 minute, which was sufficient to provide the frequency resolution (0.78 Hz) used in the subsequent analyses.

DAC in-house software operating on a DEC VAX 8300 coupled with a Numerix MARS 432 array processor was used to convert the digitized time series data into auto- and cross-spectra for the various measurement locations, with respect to the appropriate reference transducer. These spectra were further processed to meet the requirements of subsequent analyses or to provide graphic output for presentation purposes.

Sound intensity measurements were made with a Norwegian Electronics type 830 Real Time Analyzer with a type 213 sound intensity probe. Sound intensities and sound pressures in one-third octave bands were measured over 43 surface areas within the FARF cabin, as shown in Figures 8 and 9. Note that the sidewall scans did not include the window areas, which were measured separately. For each measurement the probe scanned each surface for 30 seconds, at a distance of approximately 4 inches. From the measured data, sound power levels and pressure-intensity indices were computed.

TABLE 1. EXCITATION LEVELS FOR SELECTED TESTS

Excitation Source	Test/Excitation Level	
	Baseline Configuration	Quiet Cabin Configuration
Speaker	A1 A2 = A1 + 7 dB	A1* A3 = A1 - 6 dB A4 = A1 - 12 dB
Shaker	B1 B2 = B1 x 0.5 B3 = B1 x 2	B1 B2 = B1 x 0.5 B3 = B1 x 2 B4 = B1 x 0.25 B5* = B1 x 4
Speaker + Shaker	C1 = A2 + B1 C2 = A2 + B2 C3 = A2 + B3	C1 = A1 + B1 C2 = A1 + B2 C3 = A1 + B4
Speaker Array	D1 D2 = D1 - 26 dB	D1* D2 = D1 - 10 dB D3 = D1 - 16 dB

*Test levels used for the sound intensity survey

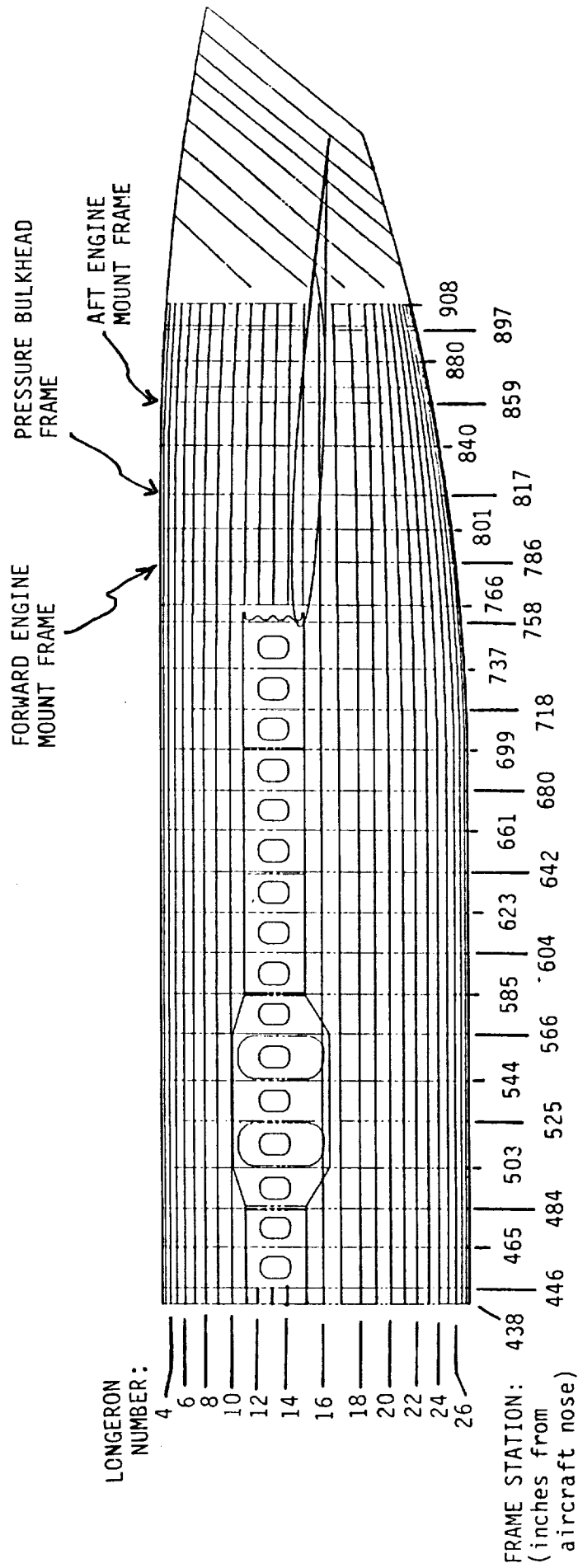


Figure 1. The DC-9 Fuselage Test Section, Showing Frame and Longeron Numbering.

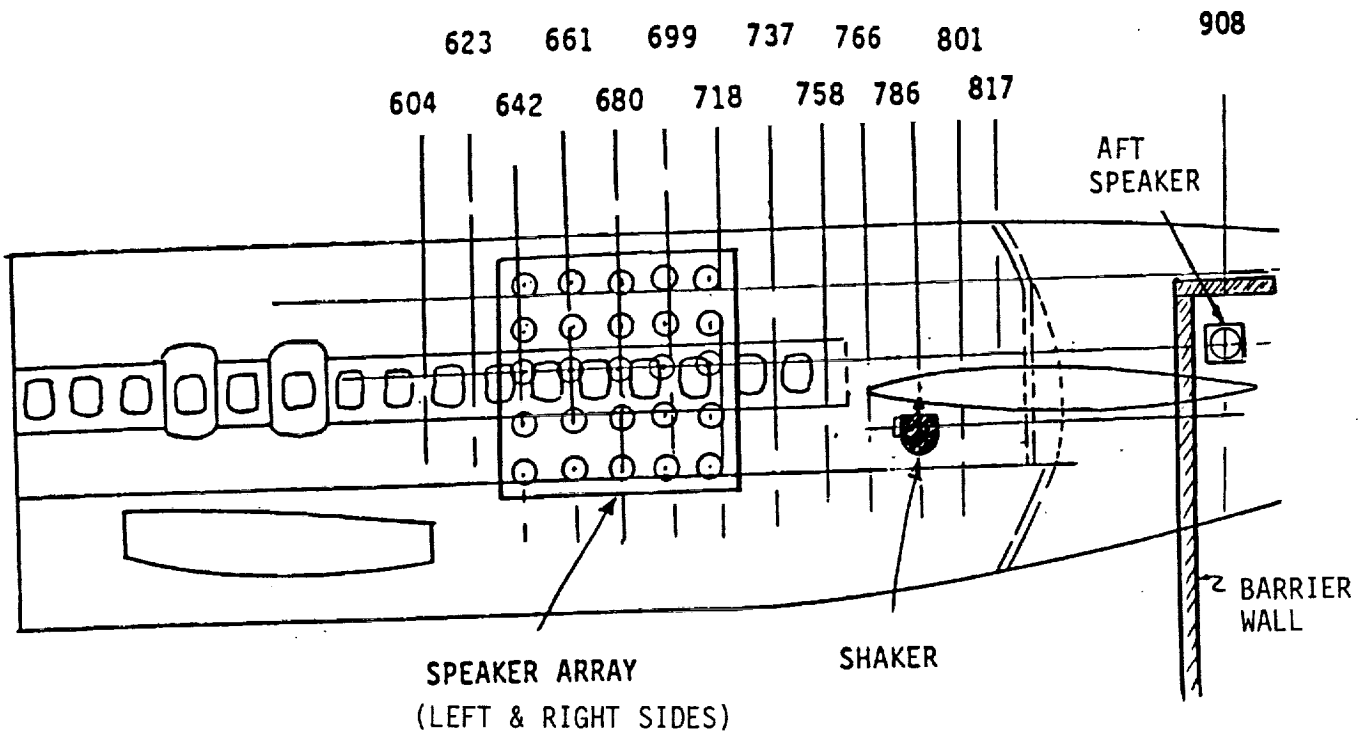


Figure 2. Noise and Vibration Source Configurations for Ground Tests.

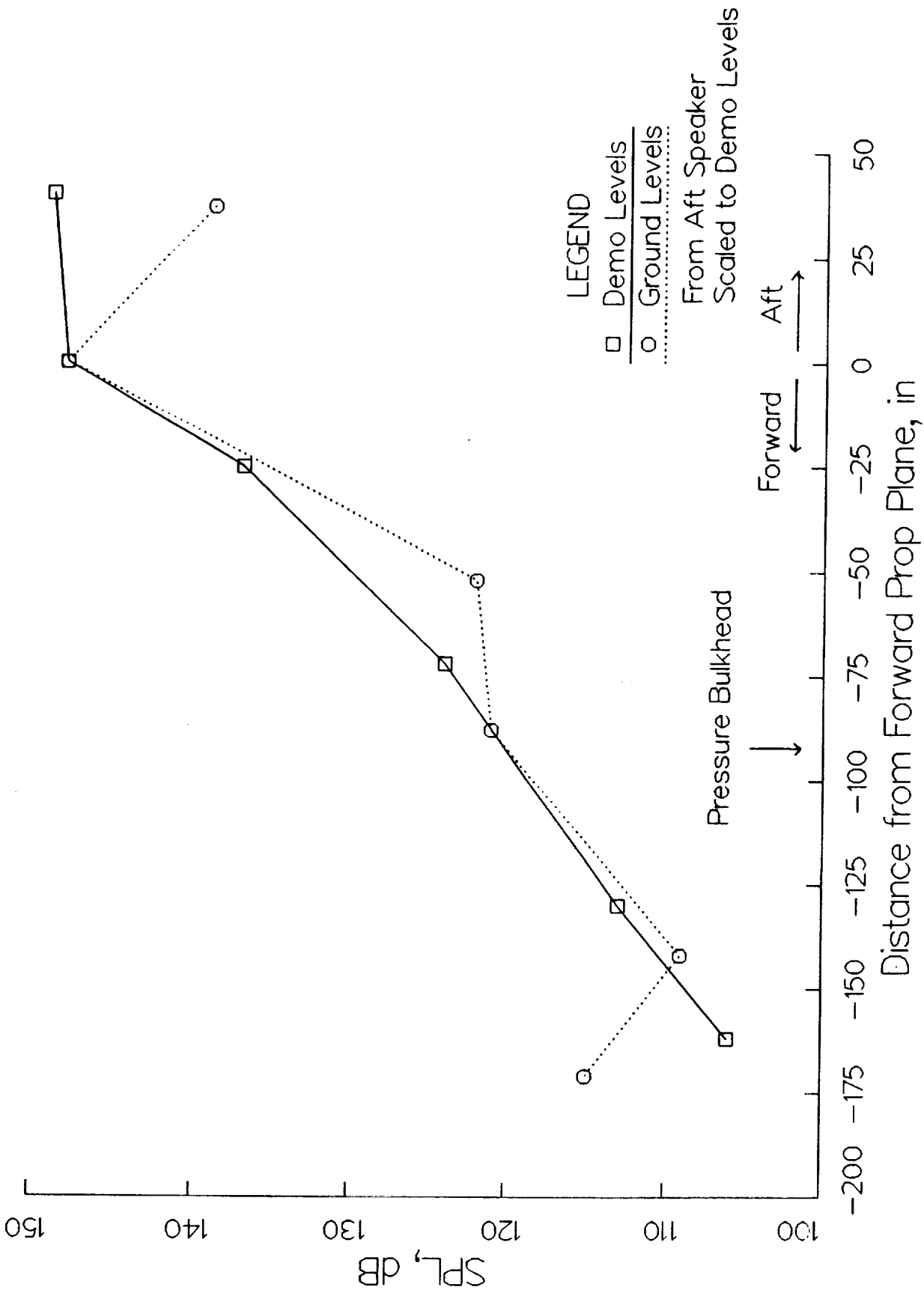


Figure 3. Comparison of the Exterior Acoustic Loads Distribution for BPF(8), Demo Vs Ground Simulation.

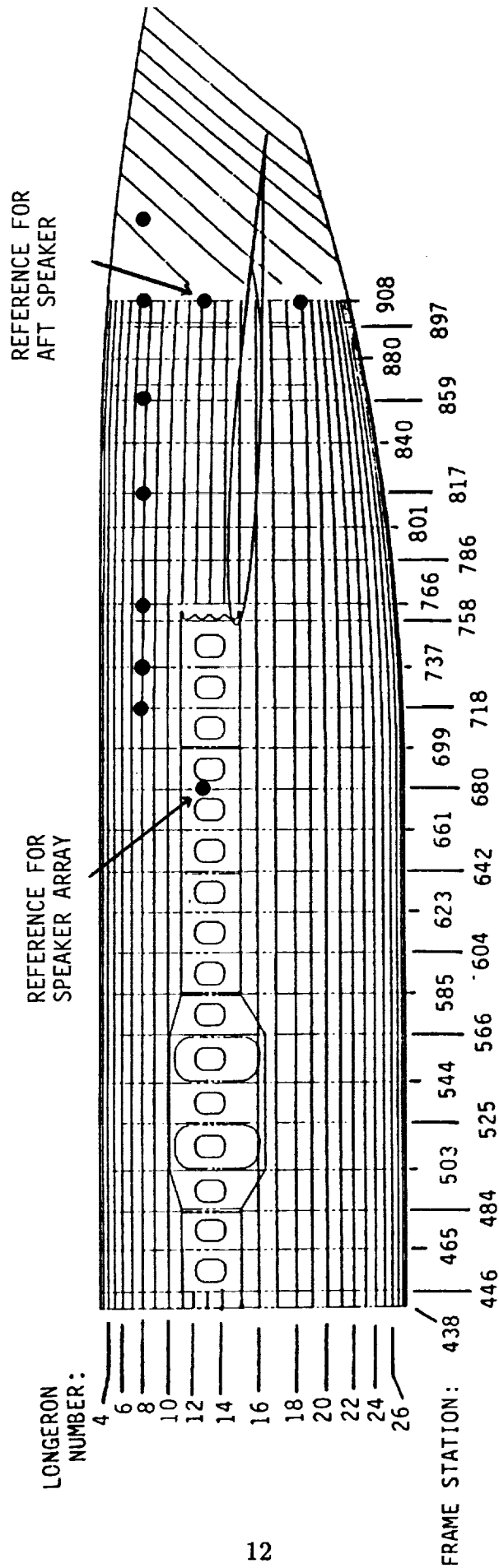


Figure 4. Exterior Microphone Locations.

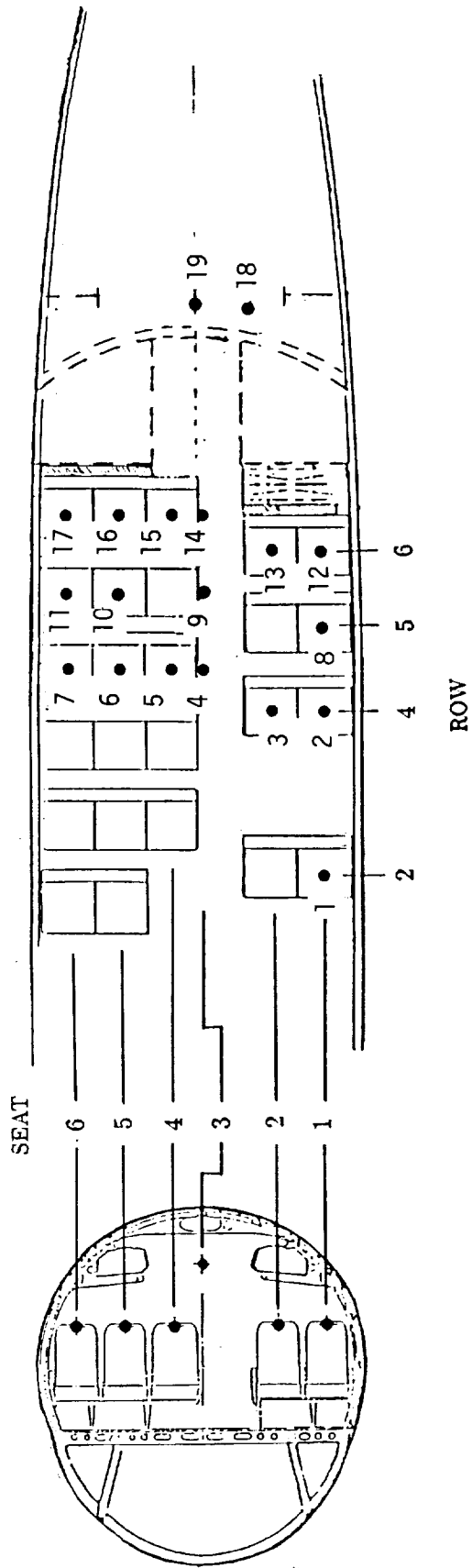


Figure 5. Cabin and Aft Section Microphone Locations.

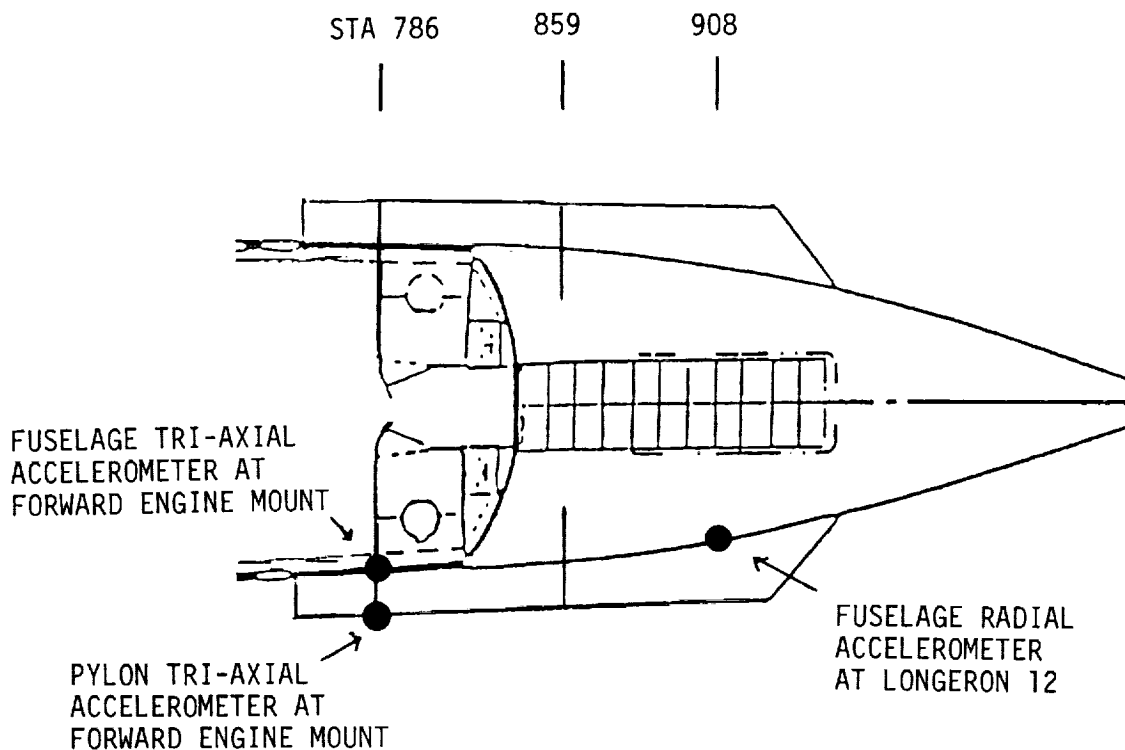


Figure 6. Location of Pylon and Fuselage Accelerometers.

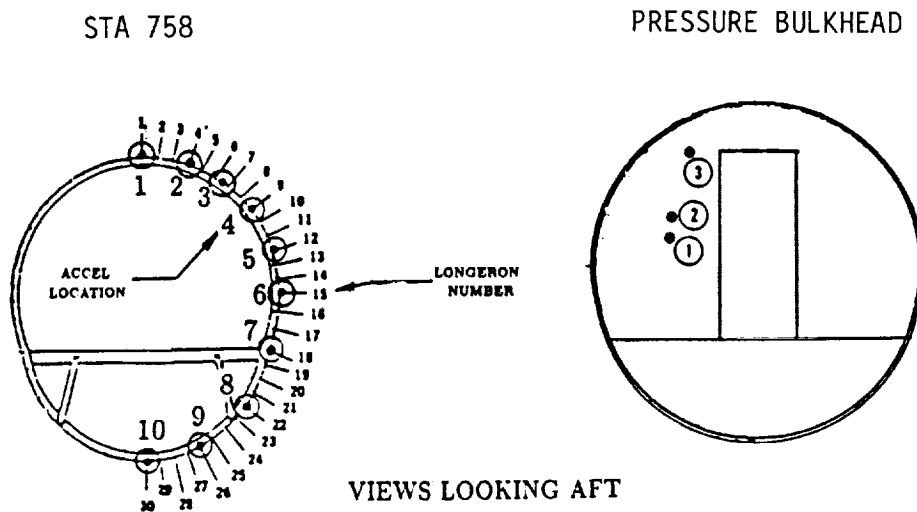


Figure 7. Frame and Aft Bulkhead Accelerometer Locations.

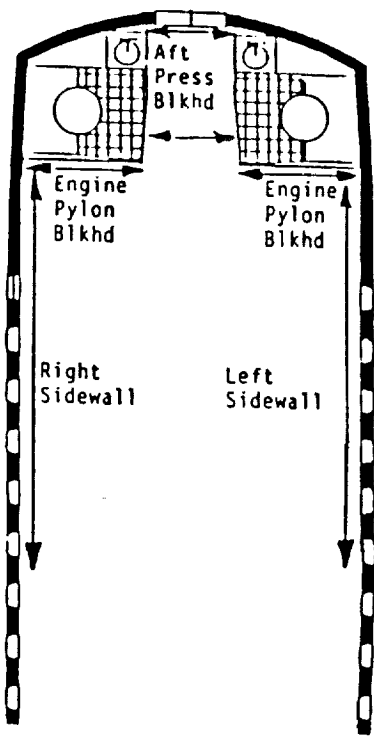
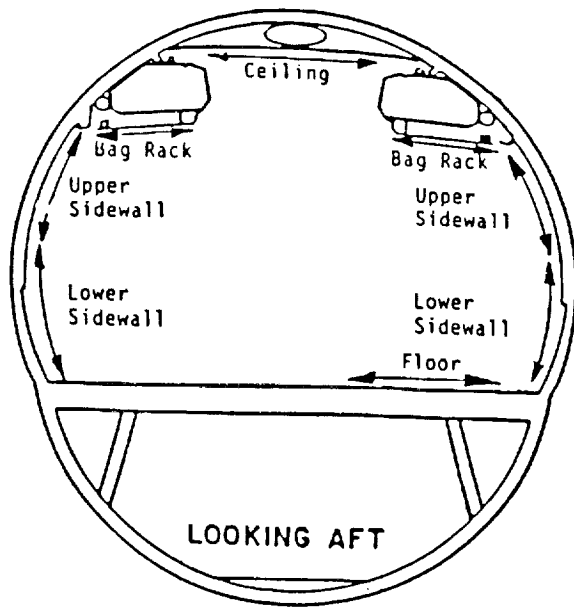


Figure 8. Sound Intensity Survey Area.

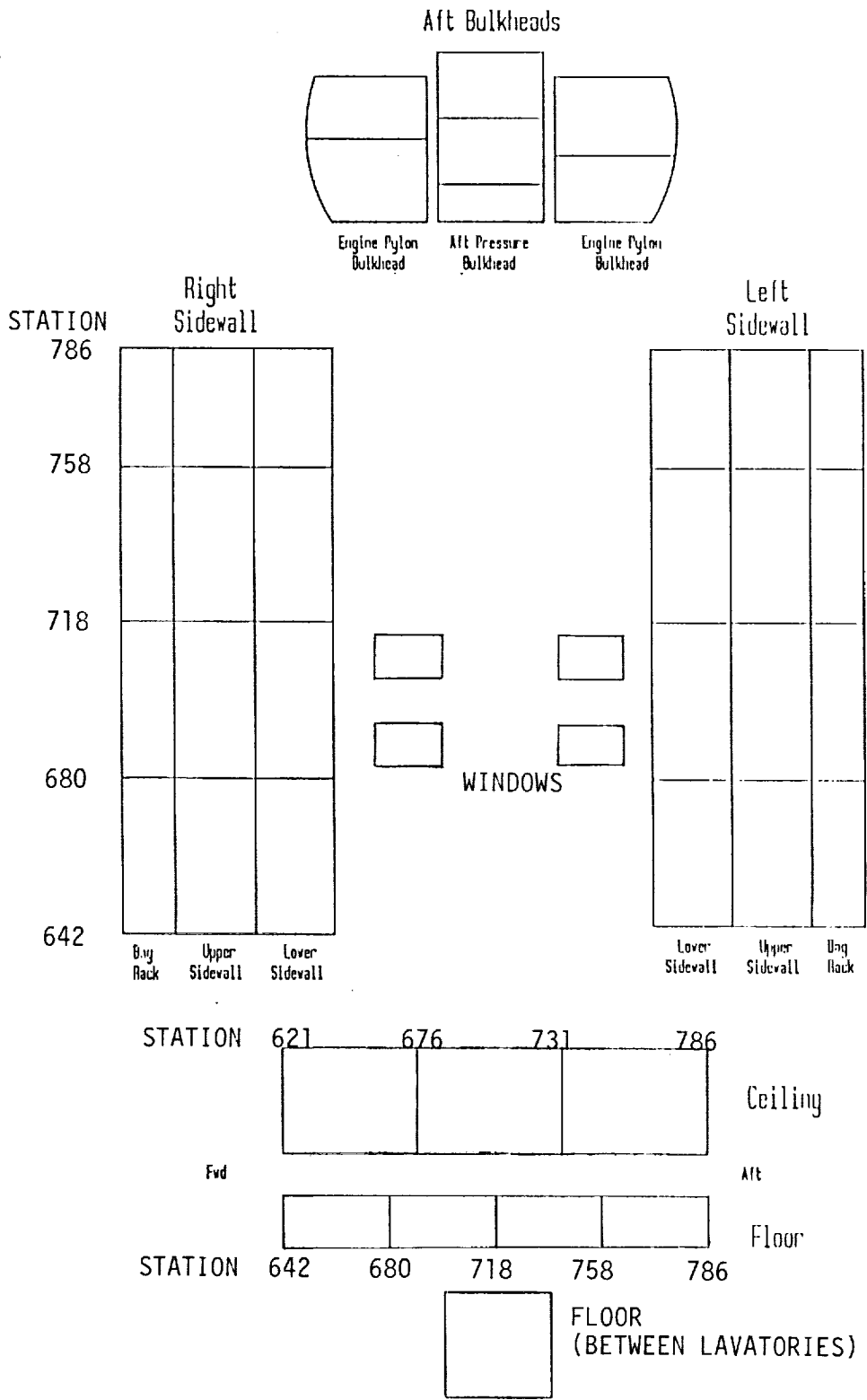


Figure 9. Location of Sound Intensity Survey Grids.

3 Ground Test Results

This section summarizes the results of the ground tests. Measured interior noise levels and acceleration levels are presented in the first two subsections for the various types of excitations, for the Baseline and Quiet Cabin Configurations. The sound intensity survey results are presented in the last subsection.

To facilitate comparisons of cabin noise and fuselage vibration levels among test points, selected data have been normalized based on source input levels. The noise and vibration levels of individual tones resulting from speaker excitation have been normalized to the following (arbitrary) noise levels, measured at the reference exterior microphone (see Figure 4): 113 dB for BPF(8) and BPF(10), and 103 dB for 2BPF(8), which are the excitation levels used in Test A1. The noise and vibration levels of individual tones resulting from shaker excitation have been normalized to the following (arbitrary) rms acceleration levels, measured at the reference pylon vertical accelerometer (see Figure 6): 0.1 g for BPF(8), BPF(10), and UN1, and 0.05 g for 2BPF(8), which are the excitation levels used in Test B1. These normalizations assume a 6 dB change in noise level for a factor of 2 change in acceleration, and vice versa.

Except for the tests involving variations in engine speed, all the tonal data reported in this section are based on an engine speed of 1260 rpm, resulting in a BPF(8) of 168 Hz and a BPF(10) of 210 Hz.

3.1 Interior Noise Levels

3.1.1 Speaker Excitation

Figure 10 shows Baseline Configuration noise levels measured at each of the 17 interior microphone locations in the aft cabin (see Figure 5), for the BPF(8), BPF(10), and 2BPF(8) tones. Similar data are shown in Figure 11 for the Quiet Cabin Configuration. Quiet Cabin levels are seen to be generally lower than Baseline levels as might be expected, but not consistently at every seat location. BPF(8) tone levels show the smallest overall decrease with configuration change.

The two figures include data obtained from multiple excitation levels. These data show that the resulting normalized cabin noise levels are relatively insensitive (within about 2 dB) to input excitation level.

For the Quiet Cabin Configuration, Figure 12 displays the variation in cabin noise level with engine speed (i.e., with changing BPF frequency). For each tone, the maximum noise levels occurring in row 4 and in row 6 are plotted. Relatively small changes

in level can be observed in the figure.

To further explore the sensitivity of measured interior noise levels, Figure 13 presents Quiet Cabin noise levels measured at three pressurization levels. Relatively small changes in noise levels occur between 5 and 3 psi, but unpressurized conditions result in significantly different levels (usually lower) as compared to either pressurization condition. These noise level changes were first thought to be due to differences in the transmission loss through the fuselage sidewall as the characteristic resistance (density \times speed of sound, ρc) of the cabin acoustic cavity varied with pressurization level. However it will be shown in Section 4 that airborne transmission through the sidewall is not the major propagation path into the cabin for speaker excitation of the fuselage. More likely, the differences in cabin noise level with pressurization are the result of changes in the stiffness of the fuselage structure as the pressurization is varied.

Figure 14 compares Quiet Cabin noise levels resulting from tonal and broadband excitations (note that the analysis bandwidth was the same for both excitations). For the three frequencies shown the general pattern of levels among the 17 locations is comparable, but the spatial distribution of levels is more uniform for the broadband excitation than for the tonal excitation. This may indicate that the individual tones can excite the cavity modes of the cabin more easily than the broadband noise.

3.1.2 Shaker Excitation

Interior noise levels due to shaker excitation are presented in Figures 15 and 16, for the Baseline and Quiet Cabin Configurations, respectively. The noise levels of all four tones are consistently lower for the Quiet Cabin Configuration. Also the normalized noise levels due to different shaker input levels show little variability. By comparison, for the speaker tone excitation (Figures 10 and 11), the variability of the normalized cabin noise levels with excitation levels is slightly higher and the noise levels for the Quiet Cabin Configuration are not consistently lower than for the Baseline Configuration.

The variation in tone noise level with engine speed for the Quiet Cabin Configuration is shown in Figure 17. The maximum levels in row 4 and row 6 are seen to vary only slightly with rpm (and tone frequency), similar to the results for speaker excitation.

Pressurization effects on Quiet Cabin noise levels are shown in Figure 18. Here, there is somewhat greater variation in noise level with changes in pressurization level than for the speaker excitation (Figure 13), especially for 2BPF(8) tone. It appears that proper simulation of pressurization level is important in the determination of interior noise levels due to engine-generated tones.

Quiet Cabin noise levels resulting from tonal and broadband shaker excitation are shown in Figure 19. These data show trends comparable to those of Figure 14, that is,

that the general pattern of levels is similar, but the spatial distribution is more uniform under broadband excitation.

3.1.3 Speaker Plus Shaker Excitation

Interior noise levels measured in the Quiet Cabin Configuration under combined speaker and shaker excitation are shown in Figure 20. For these test points, the input level of the speaker was kept constant while the input level of the shaker varied by a factor of four. (Note that because of the combined inputs, it was not possible to normalize the data in this figure.)

The figure shows a general trend of decreasing interior noise levels as the shaker input level is decreased from Test C1 to Test C3 (see Table 1 for a summary of speaker and shaker input levels for each test); this trend is particularly clear for BPF(8). Since the speaker level is fixed, it can be deduced that interior levels are dominated by shaker excitation if the noise levels decrease by 6 dB as the shaker input is halved. In contrast, it can be deduced that the interior levels are dominated by speaker excitation if the noise levels remain constant as the shaker input varies. On this basis, it appears that the interior levels for Test C1 are dominated by the shaker tones, while the interior levels for Test C3 are dominated by the speaker tones. Indeed, Test C1 levels are comparable to Test B1 levels, while Test C3 levels are comparable to Test A1 levels, for all three tones. Thus, for combined speaker and shaker excitation (as occurs during actual flight conditions), if the excitation levels are comparable to those used in these tests it can be seen that cabin noise levels arise from a combination of airborne and structureborne sources.

Figure 21 examines the variability in interior noise levels for differences in the relative phase between the speaker and shaker inputs for BPF(8) tones. Test C2 inputs were used for this comparison. The figure does not show large or systematic differences in level as the phase varies.

3.1.4 Speaker Array Excitation

Noise spectra for an aft cabin microphone location for multiple excitation levels are presented in Figures 22 and 23 for Baseline and Quiet Cabin Configurations, respectively. The interior levels for a given configuration show a uniform shift in amplitude that corresponds closely with the shift in input level (see Table 1), demonstrating that the interior spectral characteristics are not sensitive to input level. Also, the reduction in level across the frequency range between the two configurations can be seen from the figures.

The effects of pressurization variation are shown in Figure 24 for Quiet Cabin interior spectra. Between 3 and 5 psi the spectral differences are negligible, however for unpressurized conditions small differences in level at certain frequencies can be observed.

It should be noted that when the speaker array excitation is added to the combined speaker and shaker excitation, the speaker array broadband noise does not affect the tone noise levels measured in the cabin. The various BPF and UN1 tone levels at each seat location when all three sources are operating were found to be identical to the corresponding levels measured for the speaker plus shaker excitation.

3.2 Acceleration Levels

3.2.1 Speaker Excitation

Acceleration levels measured at seven longeron locations on frame 758 due to speaker excitation at three BPF frequencies are shown in Figure 25 for the Baseline Configuration, and in Figure 26 for the Quiet Cabin Configuration. The magnitude of frame acceleration levels is similar for the two cabin configurations. This is not unexpected since the added treatments for the Quiet Cabin Configuration would not likely affect frame vibration. For each configuration the normalized acceleration levels are comparable for the different speaker excitation levels, indicating that the structure responds in a linear fashion to airborne excitation.

3.2.2 Shaker Excitation

Acceleration levels at the same locations resulting from shaker excitation are presented in Figures 27 and 28 for Baseline and Quiet Cabin Configurations, respectively. As in Figures 25 and 26, frame acceleration levels are similar for the two configurations. The normalized levels among tests are nearly identical for all input levels, again indicating a linear structural response.

3.2.3 Speaker Plus Shaker Excitation

Acceleration levels due to combined speaker plus shaker excitations are shown in Figure 29 for the Quiet Cabin Configuration. (Levels are not normalized because of the dual excitations.) Since the measured acceleration levels decrease from Tests C1 to C2, the shaker excitation is likely the major source of the Test C1 levels. However, since levels do not decrease in half from Tests C1 to C2, and then in half again from Tests C2

to C3, speaker excitation appears to be an increasingly important contributor to the acceleration levels. Comparison of the shaker-generated acceleration levels in Figure 28 and the speaker-generated levels in Figure 26 with the levels in Figure 29 verifies these results. It may be noted that these are the same conclusions presented above, based on review of the interior noise levels for the individual and combined excitations.

3.3 Sound Intensity Survey Results

Figures 30, 31, and 32 show the sound power levels for each scanned surface (see Figures 8 and 9), for individual speaker, shaker, and speaker array excitations, respectively. On the first two figures, power levels are listed for the 160, 200, and 315 Hz one-third octave bands. These bands contain the BPF(8), BPF(10), and 2BPF(8) tones generated by the speaker excitation (Figure 30), or the BPF(8), UN1, and 2BPF(8) tones generated by the shaker excitation (Figure 31). For the speaker array excitation (Figure 32), power levels are listed for the eight one-third octave bands from 100 to 500 Hz.

On the figures, positive values indicate energy flow from the scanned surface, while negative values indicate energy flow into the surface. Levels in parentheses indicate that the pressure-intensity index for that particular measurement is greater than 20 dB, and therefore the data are questionable.

Figure 30 shows that the surfaces radiating the highest sound power levels under speaker excitation for the BPF(8) tone are the aft pressure bulkhead and the floor between the lavatories. For the BPF(10) tone, the major surfaces include the aft pressure bulkhead, left engine pylon bulkhead, and left aft sidewall. For the 2BPF(8) tone, the aft pressure bulkhead is the major radiating surface. (Note that for this sound intensity survey, excitation levels from the speaker were too low to obtain meaningful measurements for surfaces far removed from the point of excitation. Thus the survey was limited to the aft, left side of the fuselage.)

For shaker excitation, the highest sound power levels for the BPF(8) tone (see Figure 31) were radiated by the left sidewall, the left engine pylon bulkhead, the ceiling, and the aft pressure bulkhead. For the UN1 tone the major surfaces are the left sidewall, the left pylon and aft pressure bulkheads, and the floor between the lavatories. For the 2BPF(8) tone, the major surfaces are the left pylon bulkhead, the left sidewall, the aft pressure bulkhead, the right pylon bulkhead, and the floor between the lavatories.

Under speaker array excitation (Figure 32), the left and right sidewalls are major radiating surfaces for the entire range of frequencies. The ceiling and floor are also important surfaces, particularly for the lower frequencies.

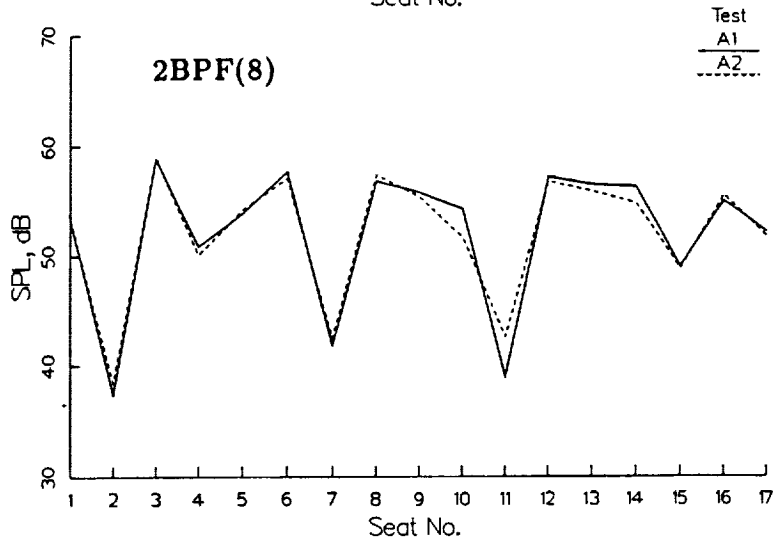
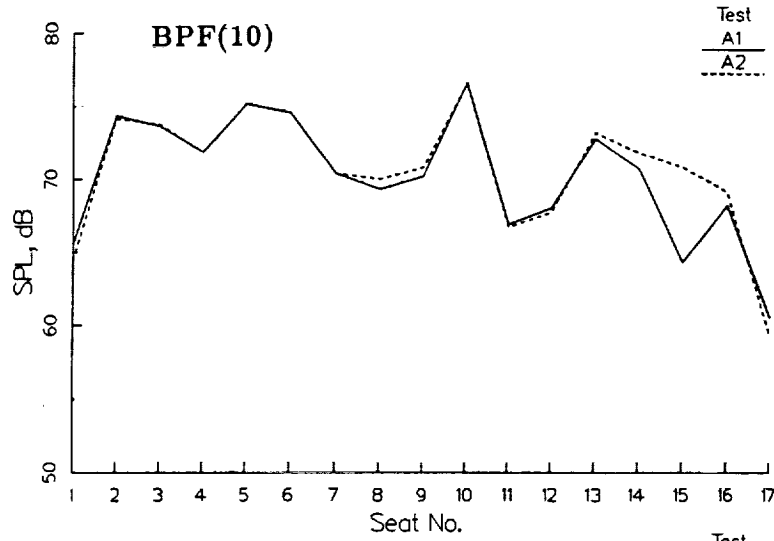
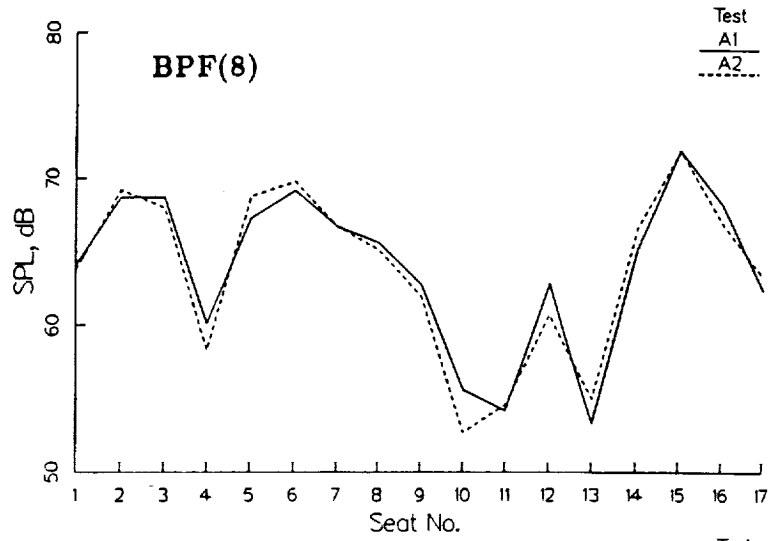


Figure 10. Normalized Cabin Noise Levels due to Speaker Excitation, Baseline Configuration.

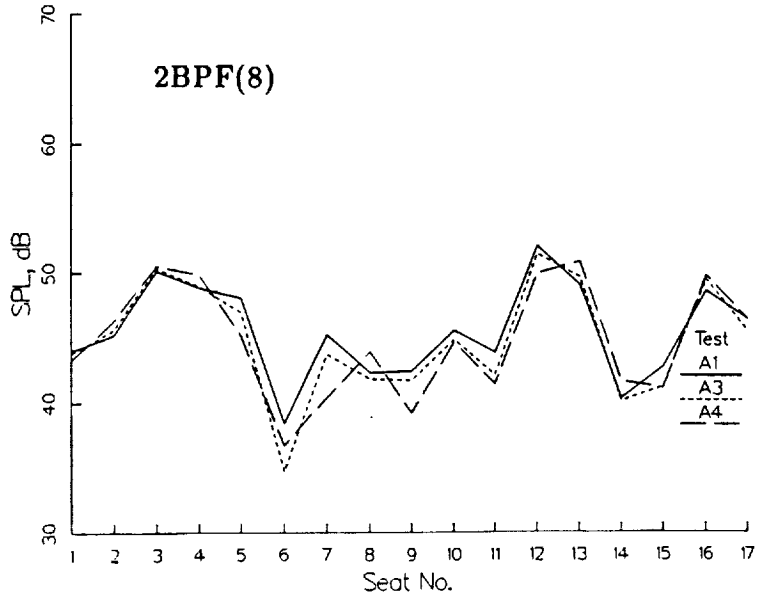
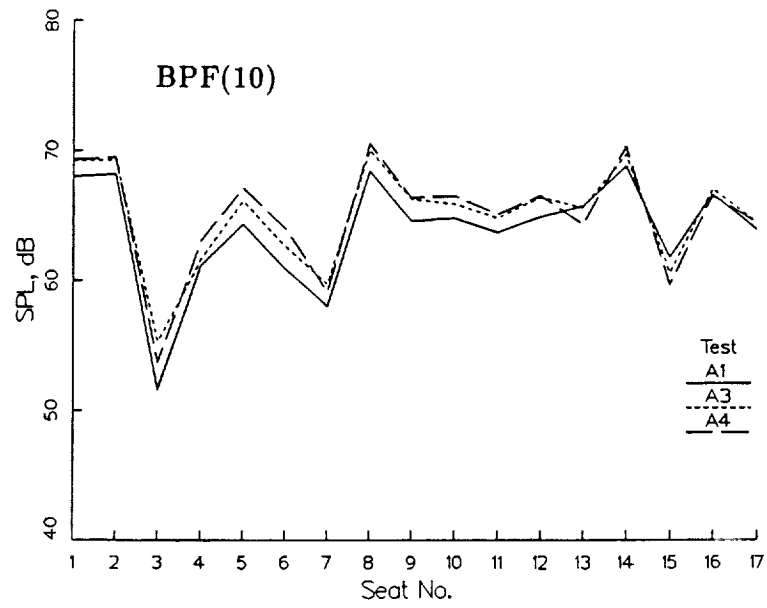
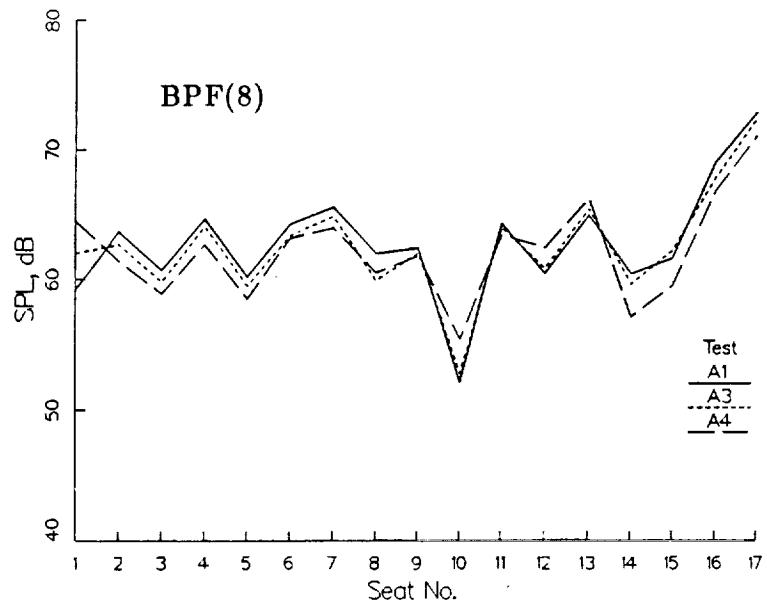


Figure 11. Normalized Cabin Noise Levels due to Speaker Excitation, Quiet Cabin Configuration.

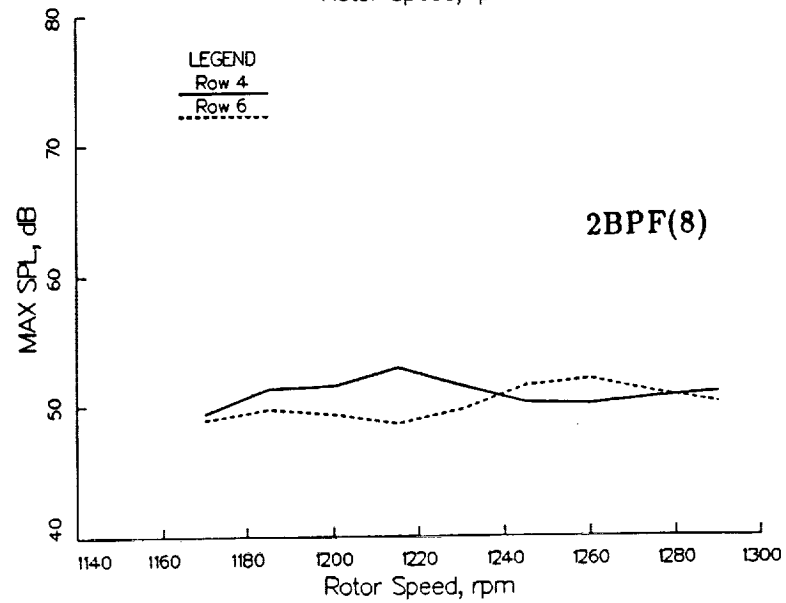
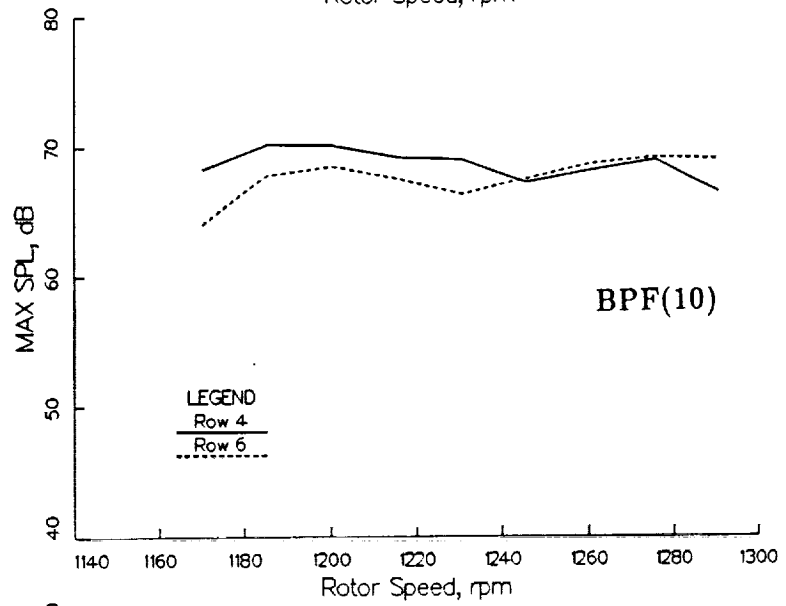
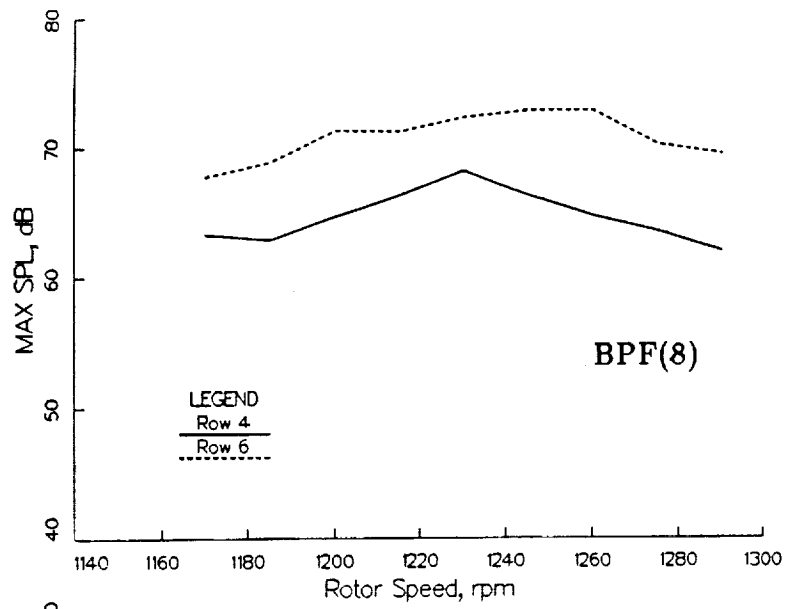


Figure 12. Variation of Maximum Cabin Noise Levels due to Speaker Excitation with Rotor Speed, Quiet Cabin Configuration.

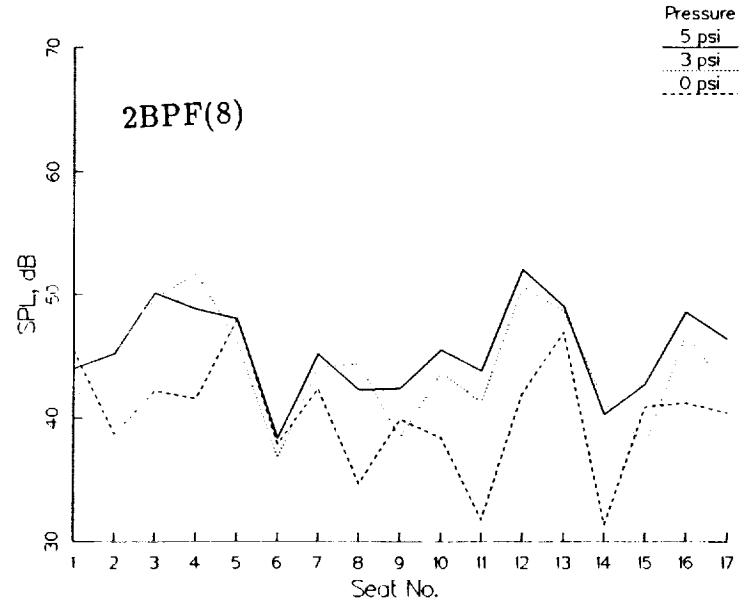
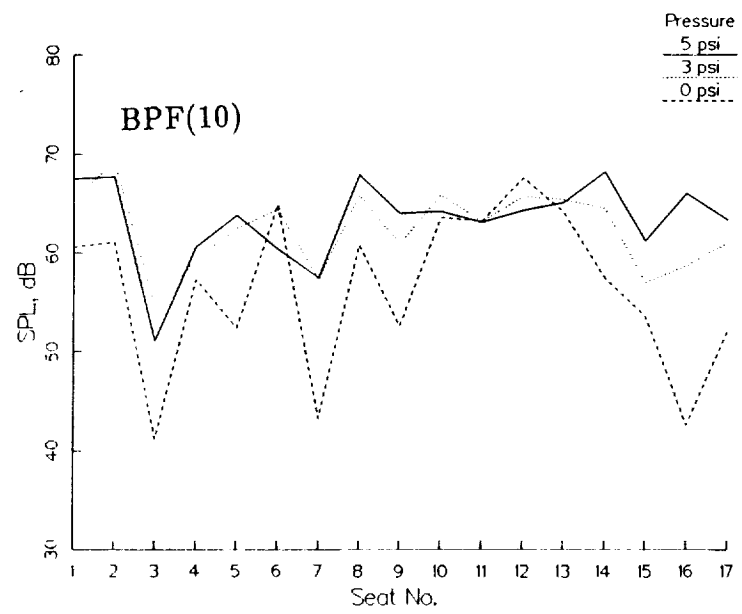
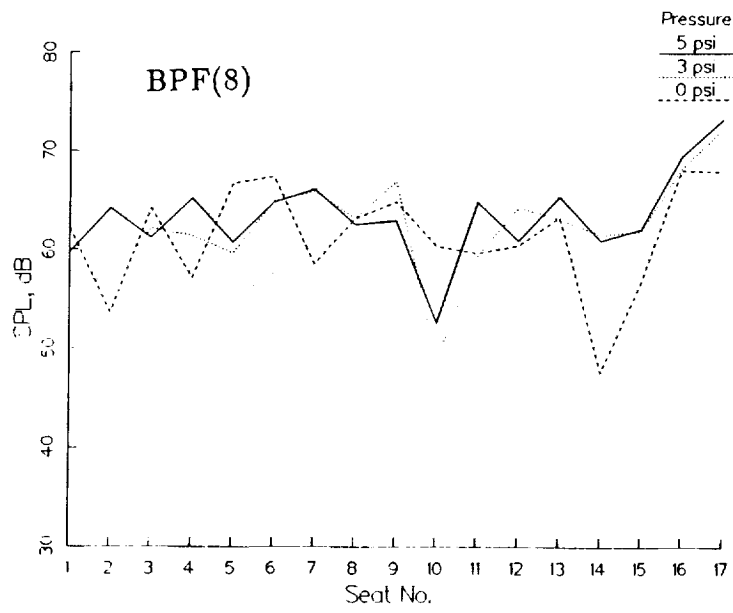


Figure 13. Effect of Pressurization on Cabin Noise Levels due to Speaker Excitation, Quiet Cabin Configuration.

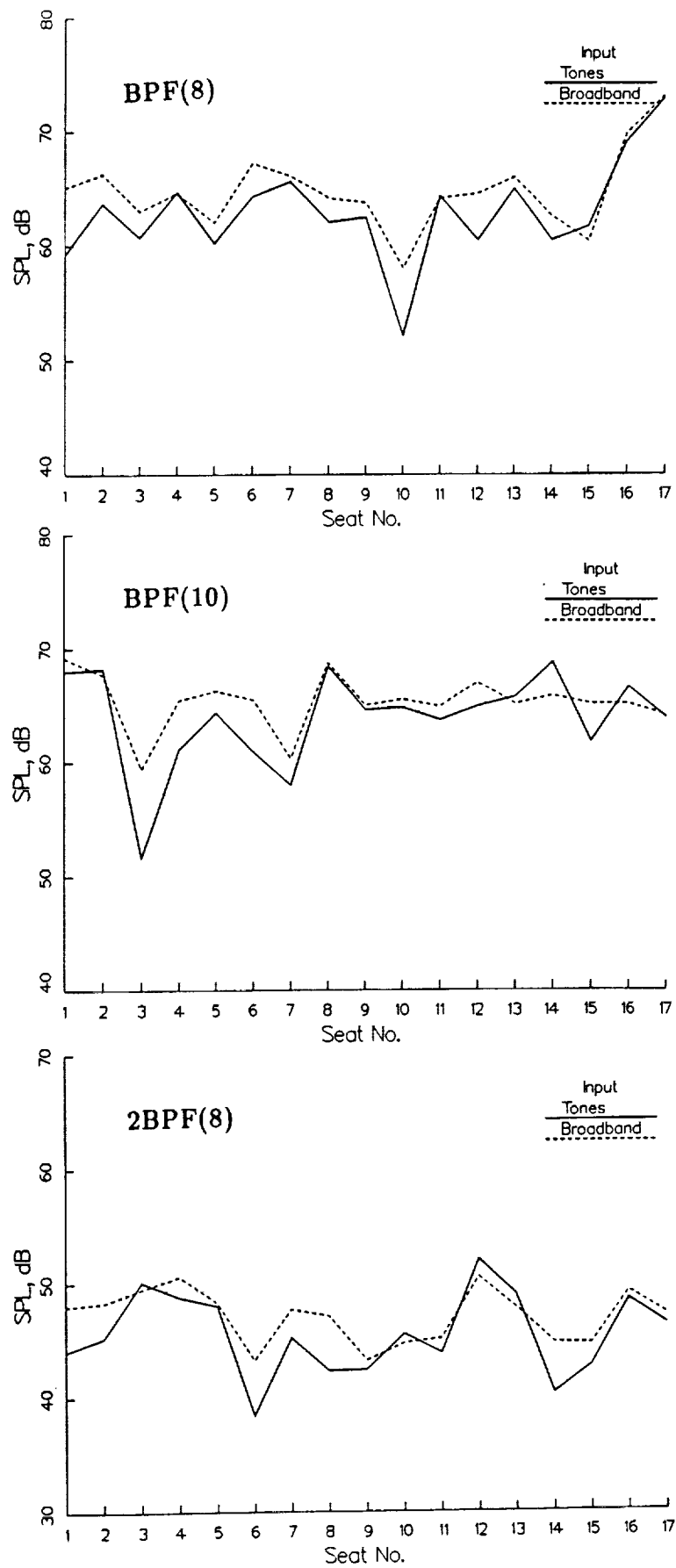


Figure 14. Comparison of Cabin Noise Levels due to Speaker Tonal and Broadband Excitation, Quiet Cabin Configuration.

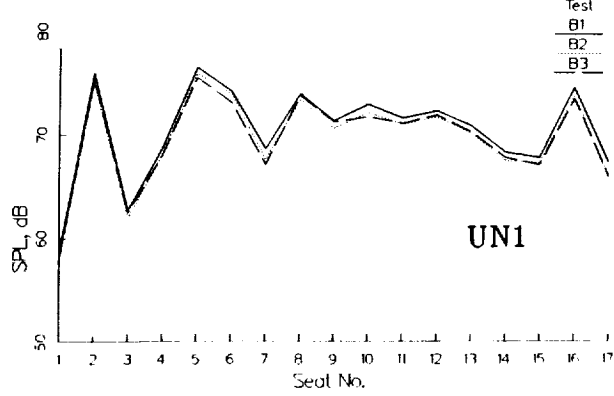
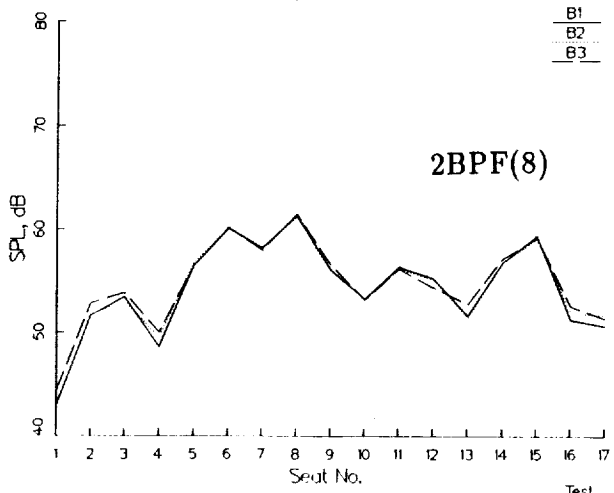
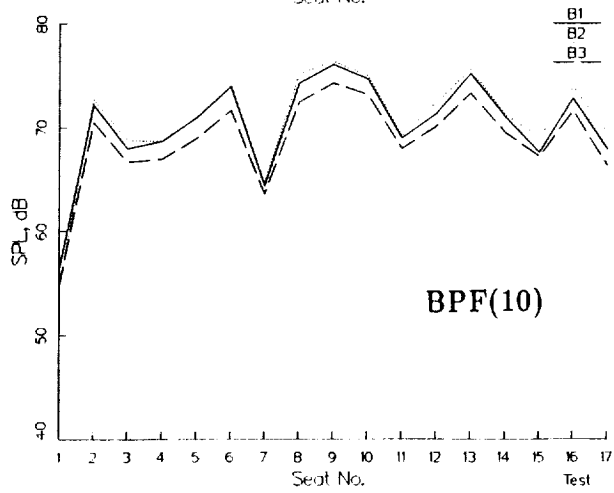
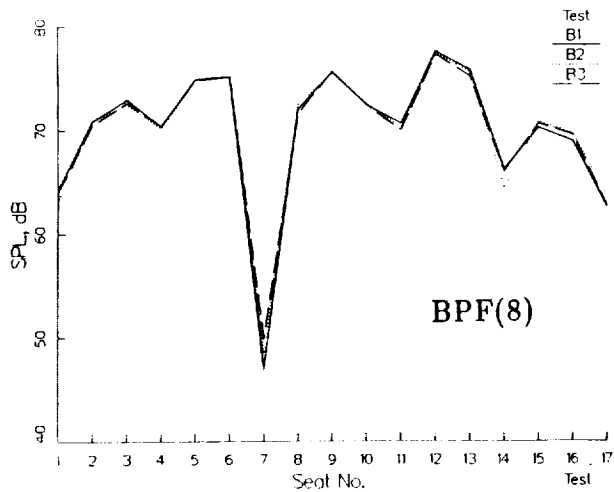


Figure 15. Normalized Cabin Noise Levels due to Shaker Excitation, Baseline Configuration.

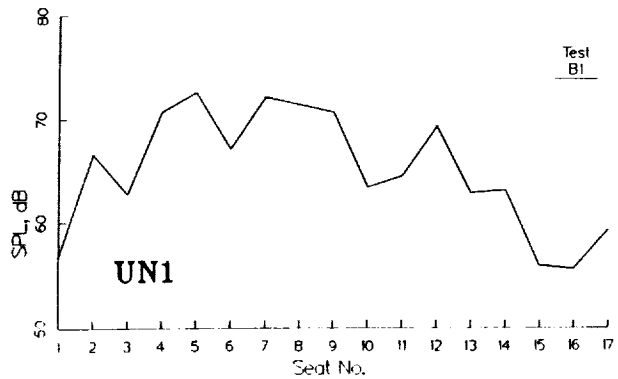
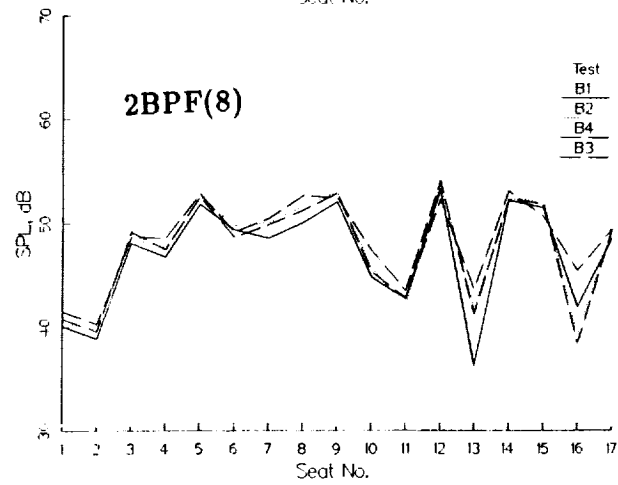
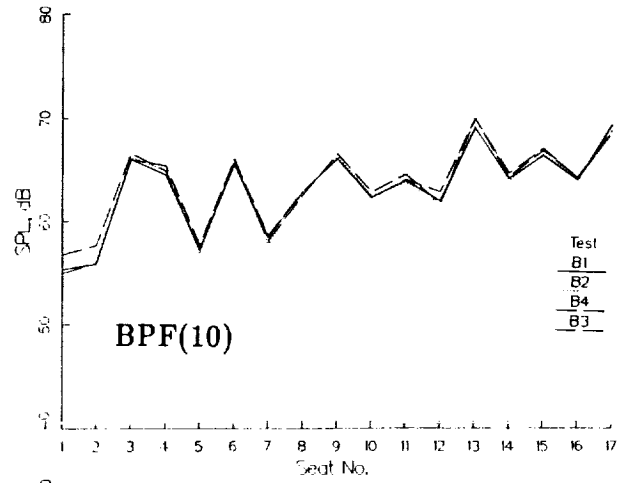
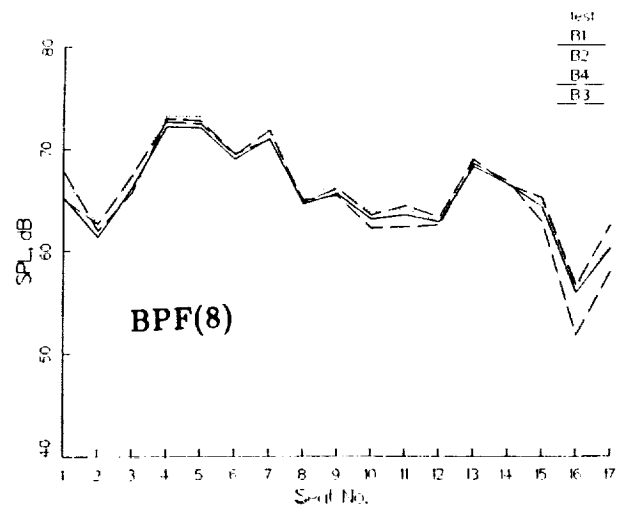


Figure 16. Normalized Cabin Noise Levels due to Shaker Excitation, Quiet Cabin Configuration.

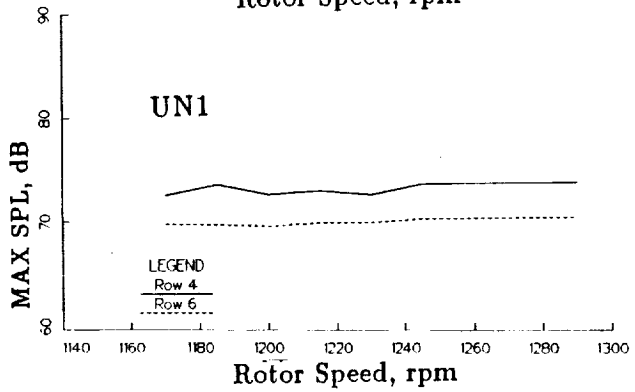
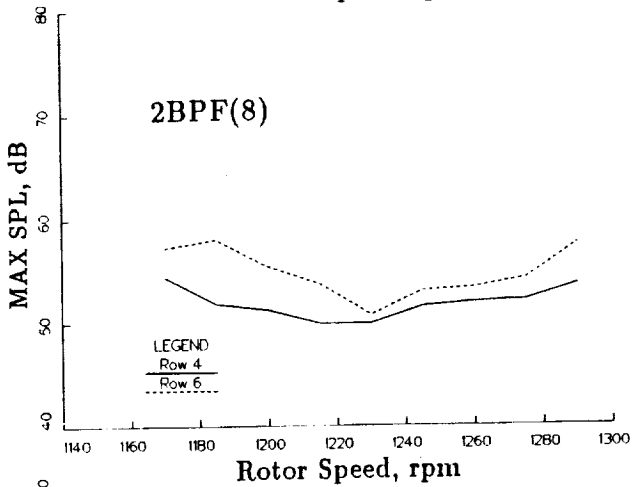
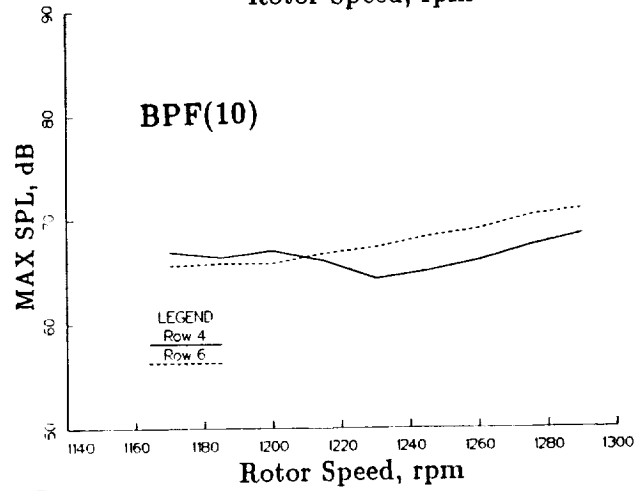
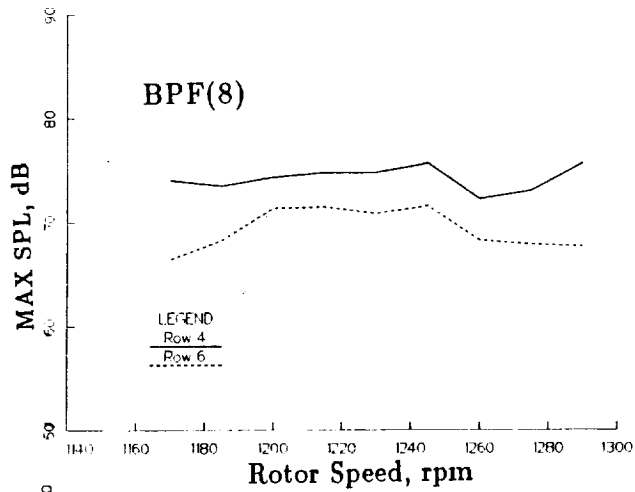


Figure 17. Variation of Maximum Cabin Noise Levels due to Shaker Excitation with Rotor Speed, Quiet Cabin Configuration.

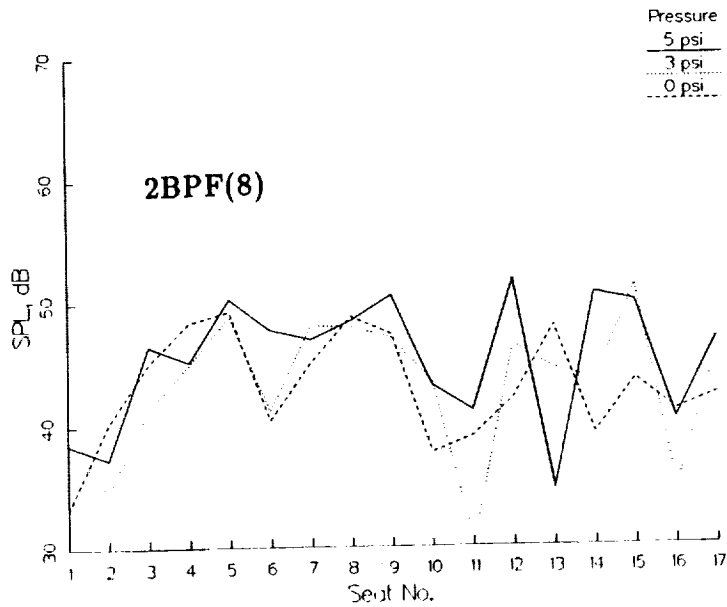
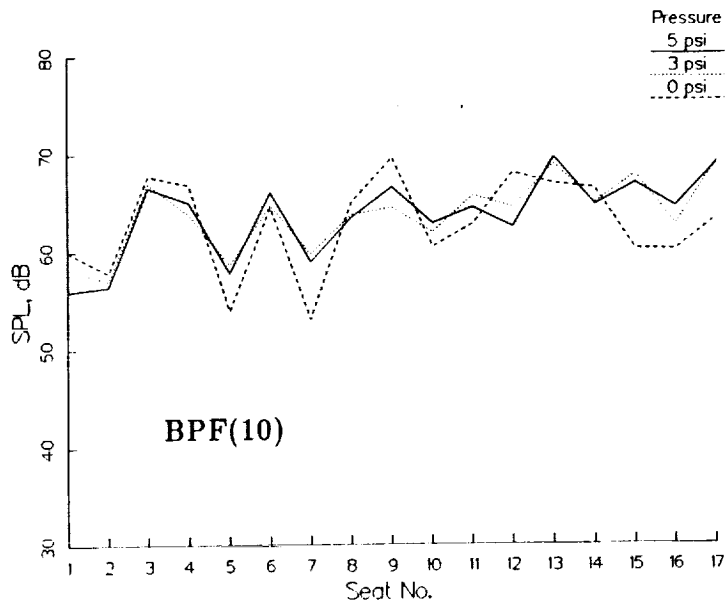
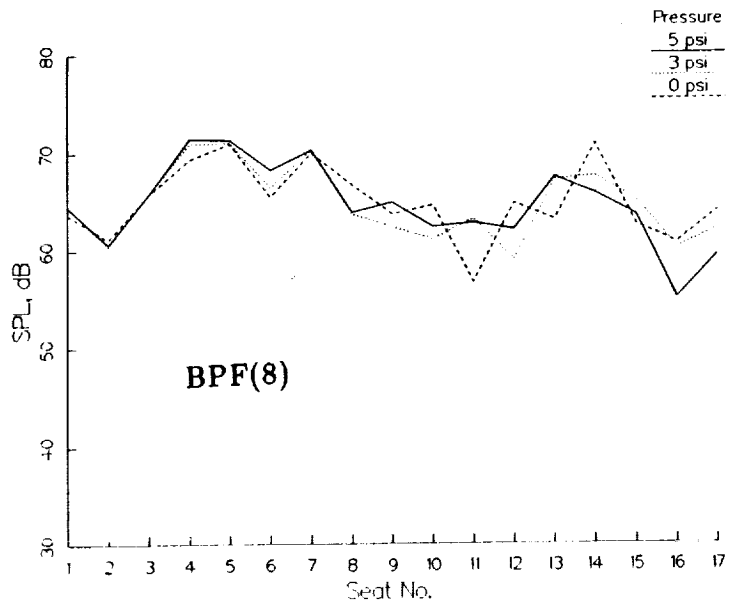


Figure 18. Effect of Pressurization on Cabin Noise Levels due to Shaker Excitation, Quiet Cabin Configuration.

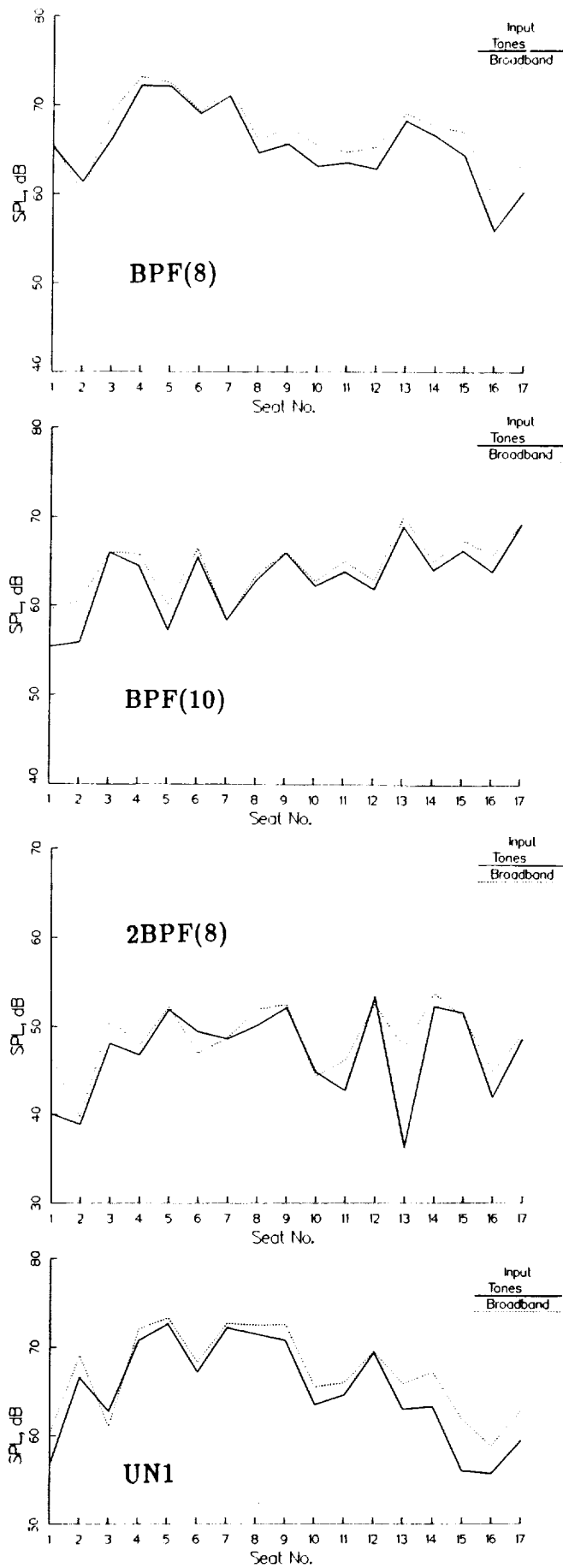


Figure 19. Comparison of Cabin Noise Levels due to Shaker Tonal and Broadband Excitation, Quiet Cabin Configuration.

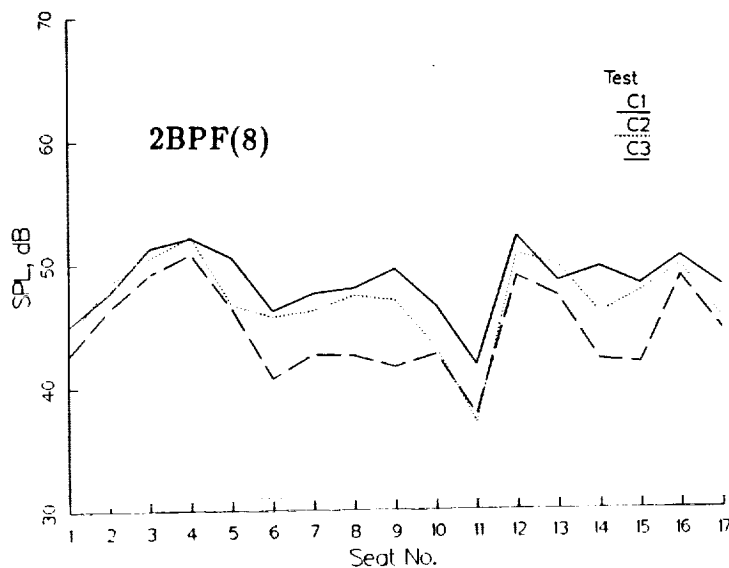
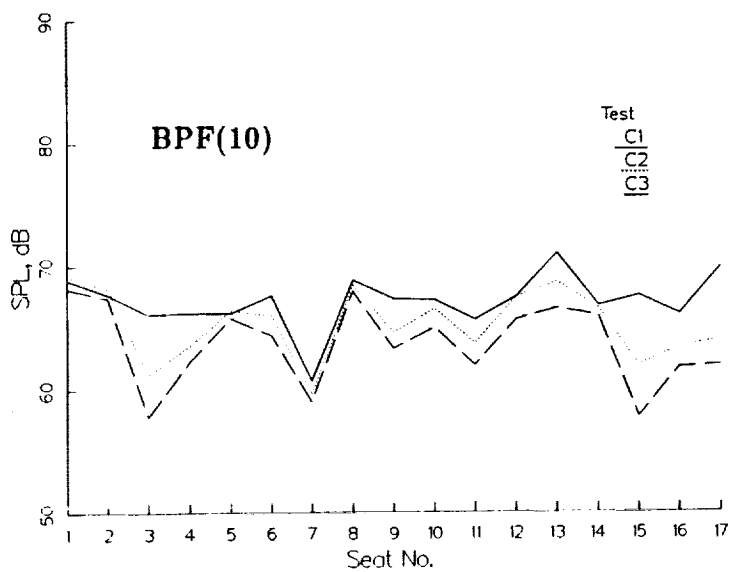
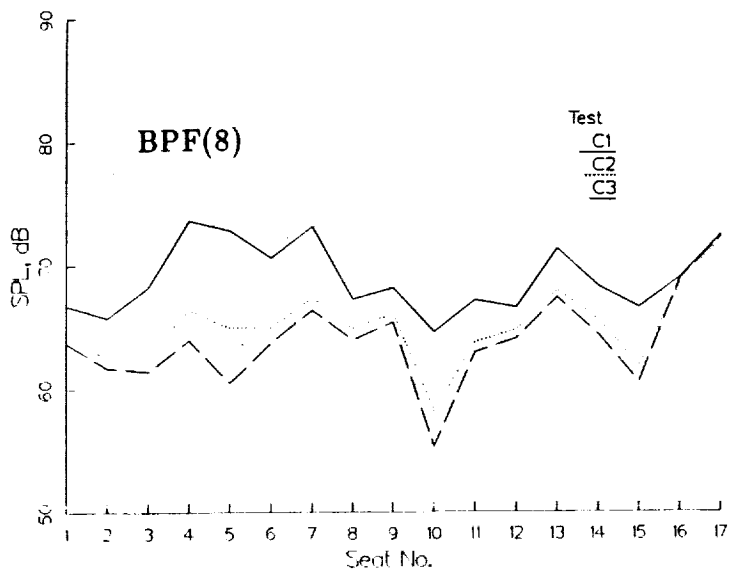


Figure 20. Cabin Noise Levels due to Combined Speaker and Shaker Excitation, Quiet Cabin Configuration.

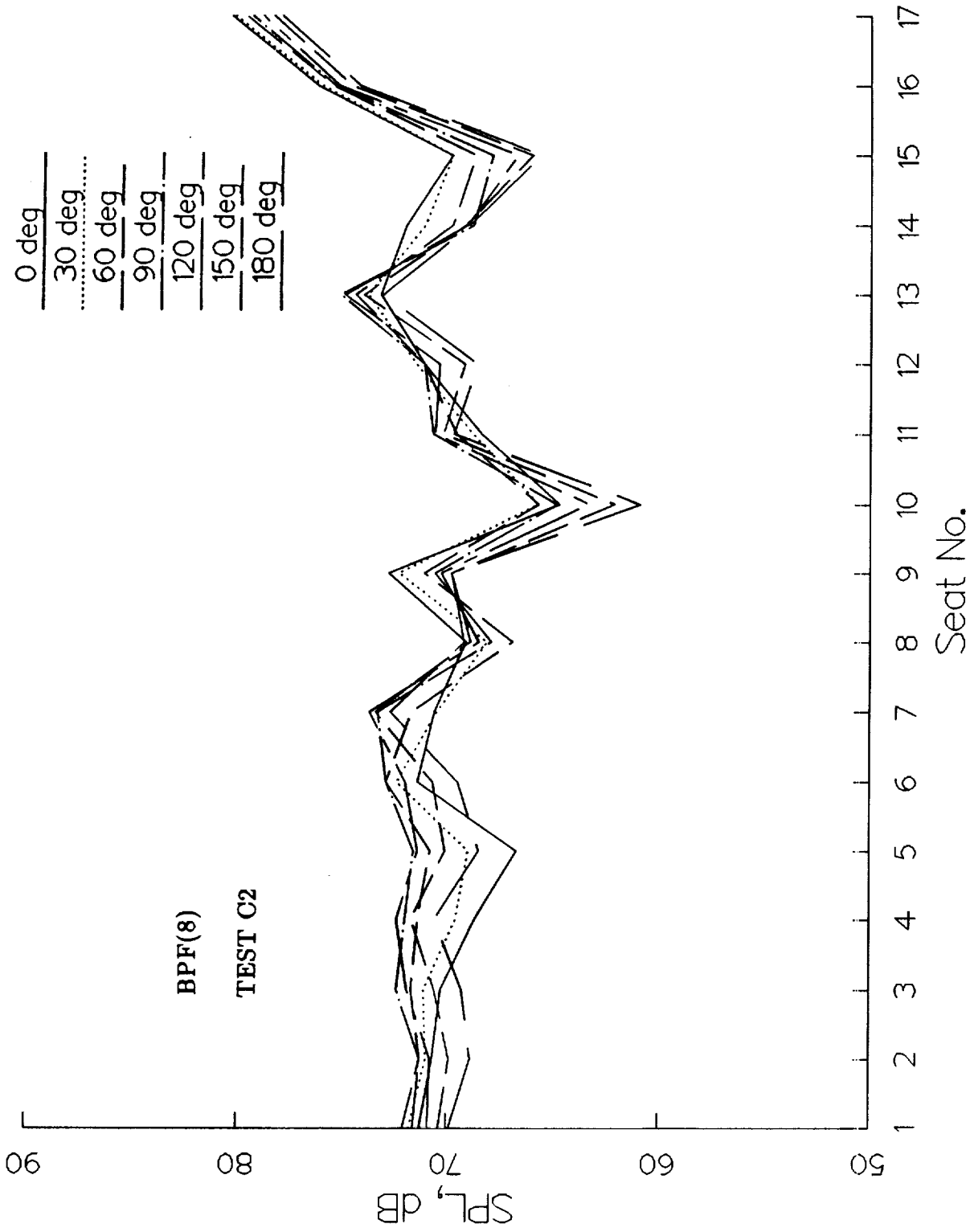


Figure 21. Effect of Variation in Relative Phase Between Speaker and Shaker Excitation on Cabin Noise Levels due to Combined Excitation, Quiet Cabin Configuration.

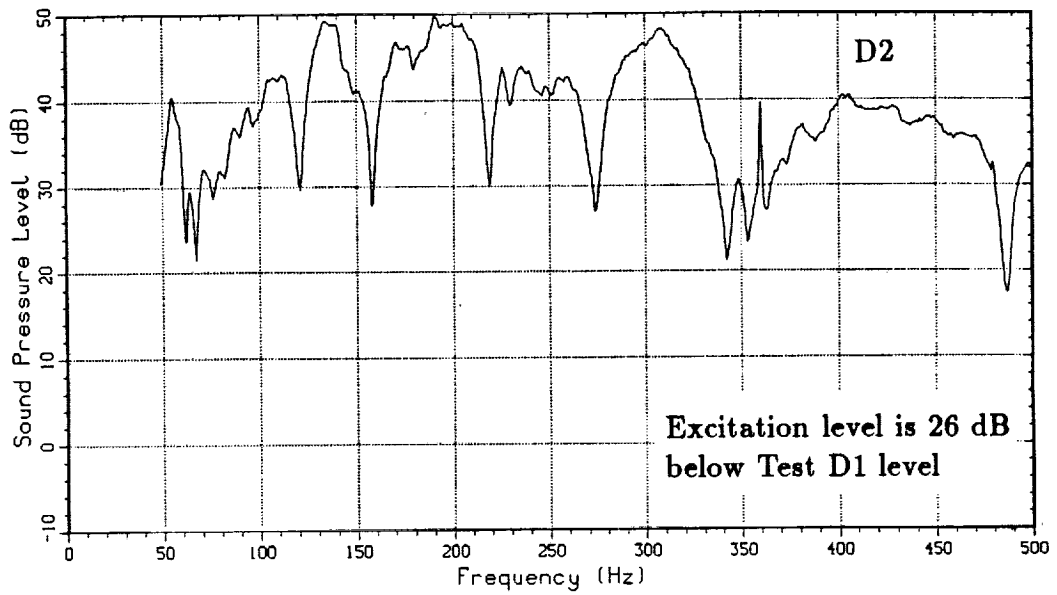
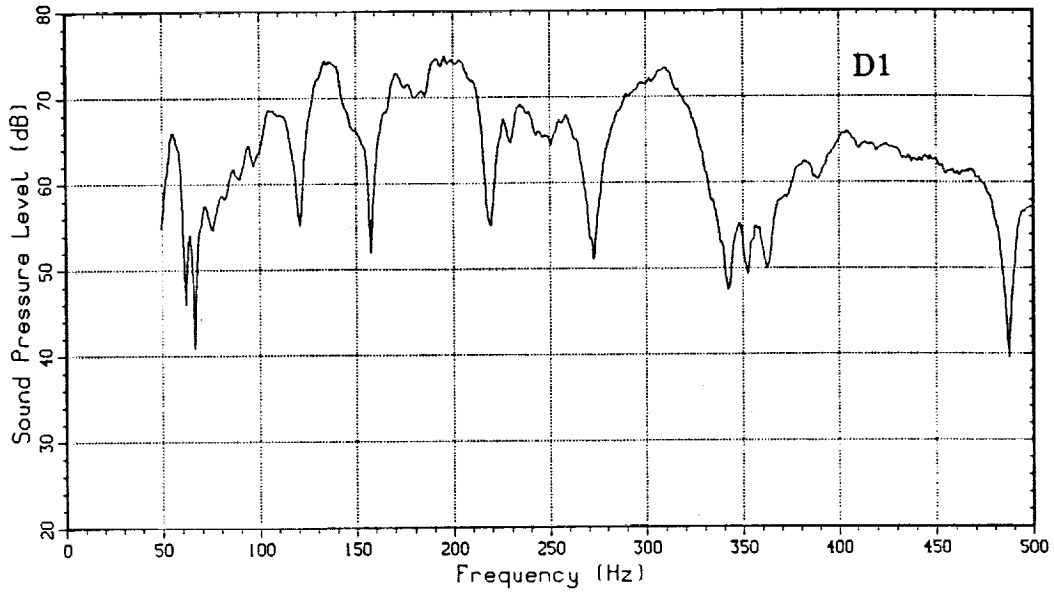


Figure 22. Noise Spectra at Seat 5, Row 5 due to Loudspeaker Array Excitation, Baseline Configuration.

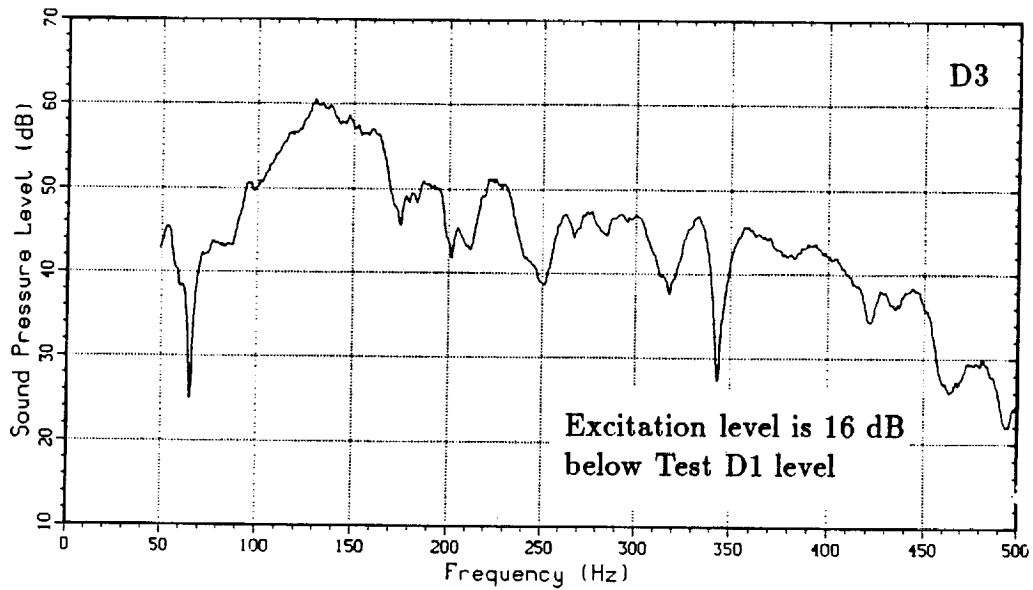
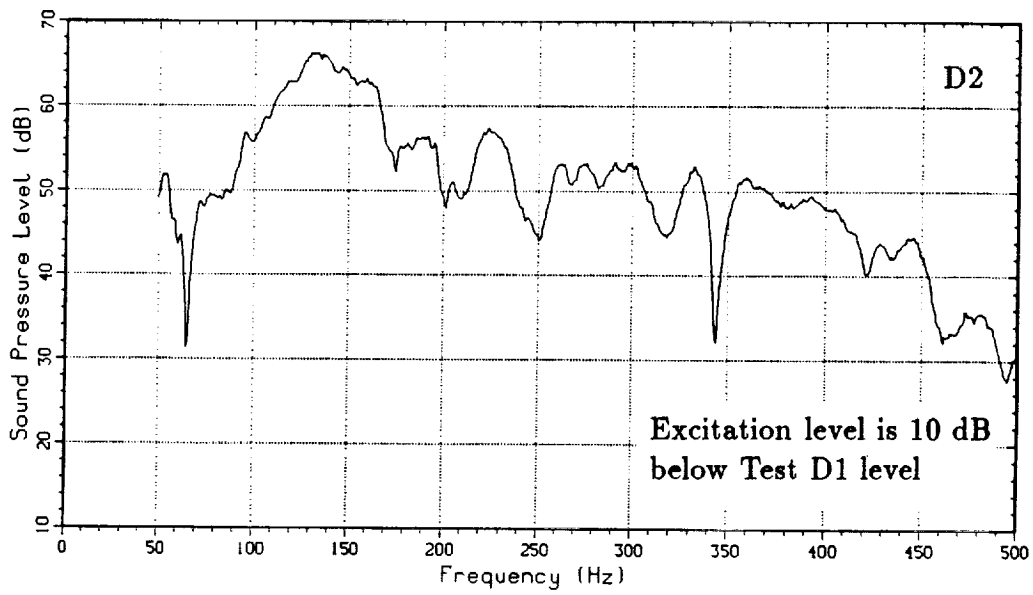
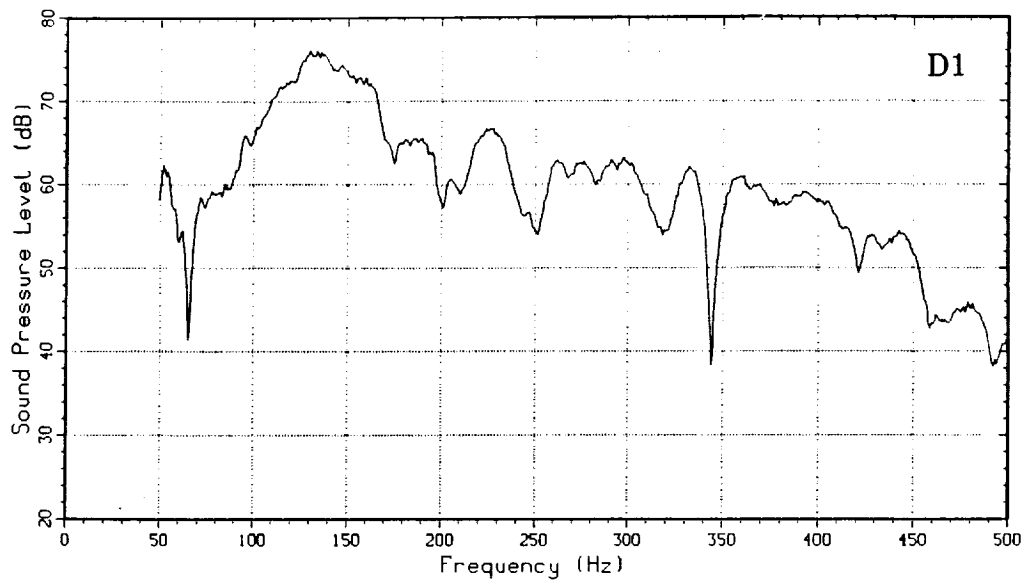


Figure 23. Noise Spectra at Seat 5, Row 5 due to Loudspeaker Array Excitation, Quiet Cabin Configuration.

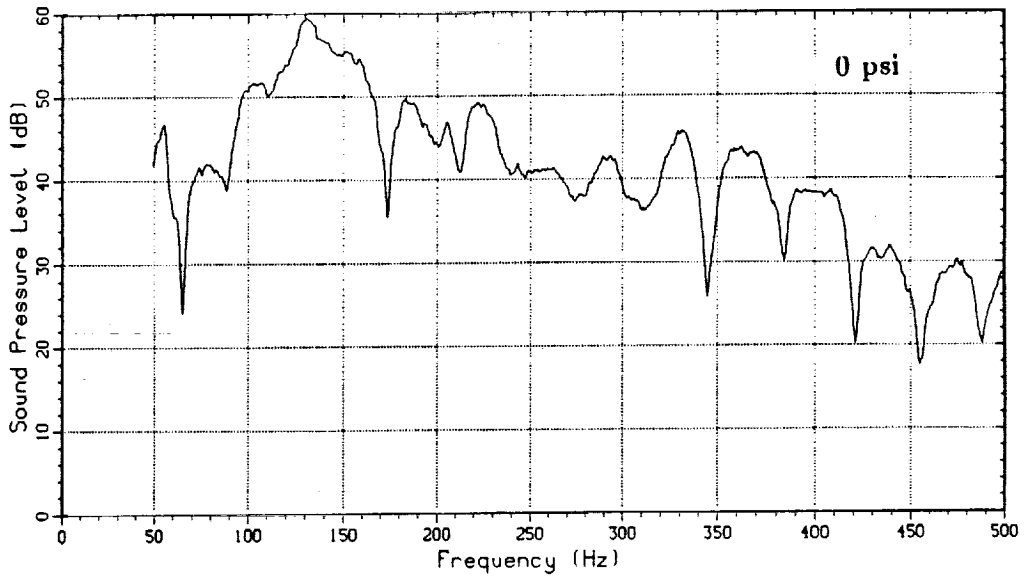
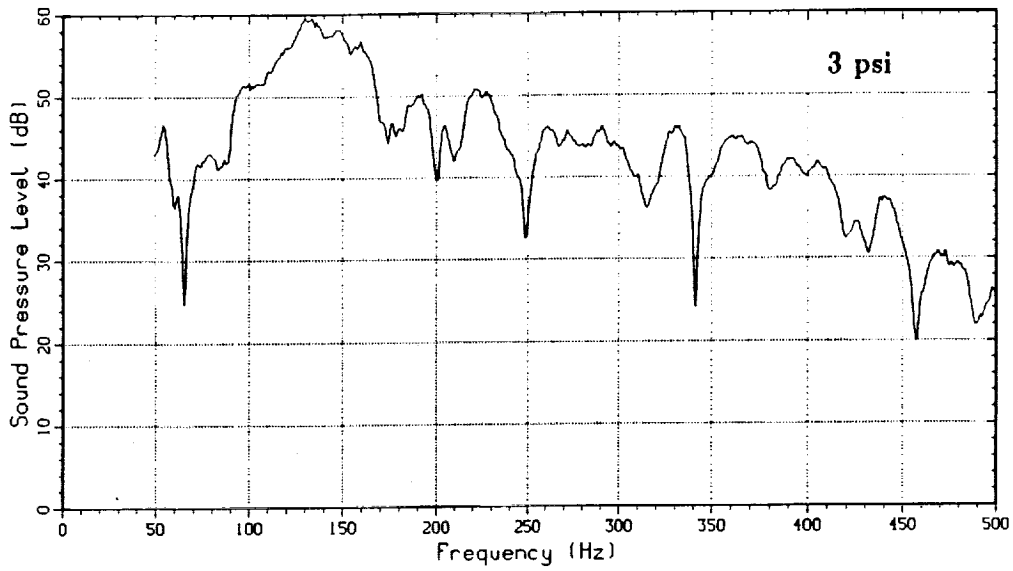
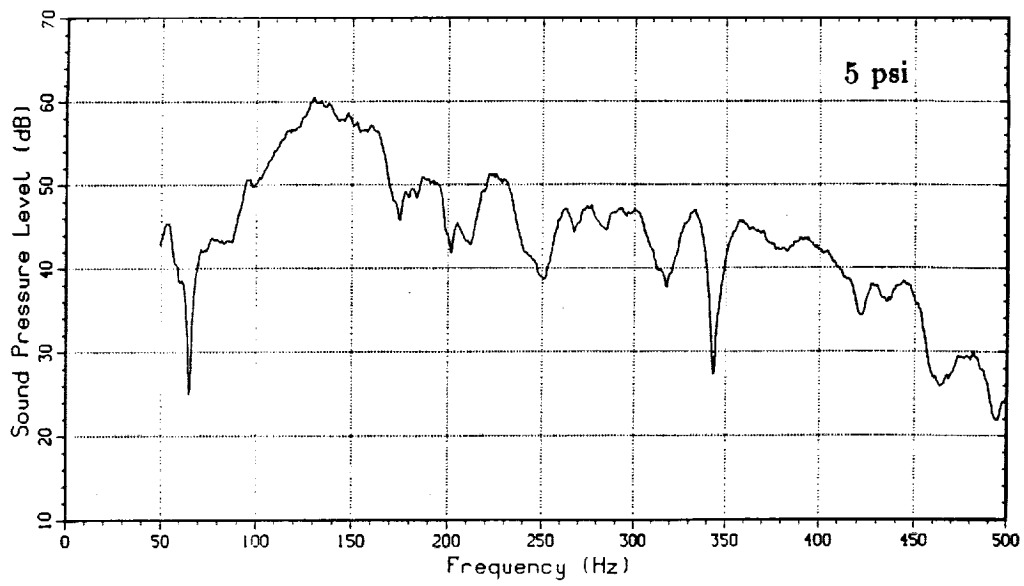


Figure 24. Effect of Pressurization on Noise Spectra at Seat 5, Row 5 due to Loudspeaker Array Excitation.

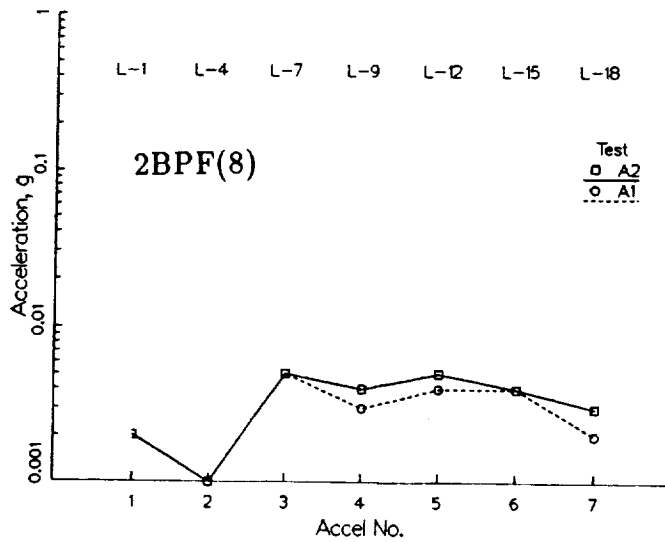
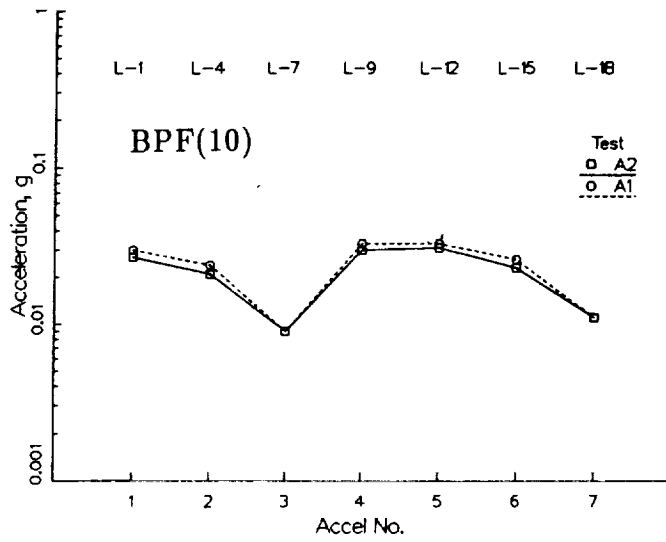
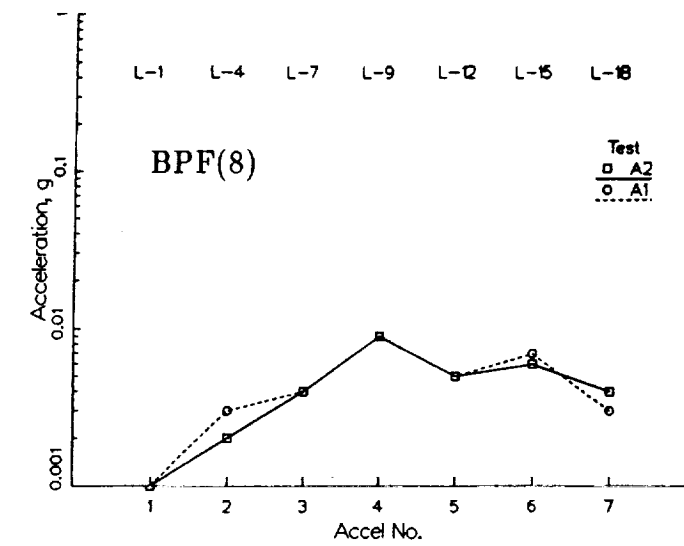


Figure 25. Normalized Frame 758 Accelerometer Levels due to Speaker Excitation, Baseline Configuration.

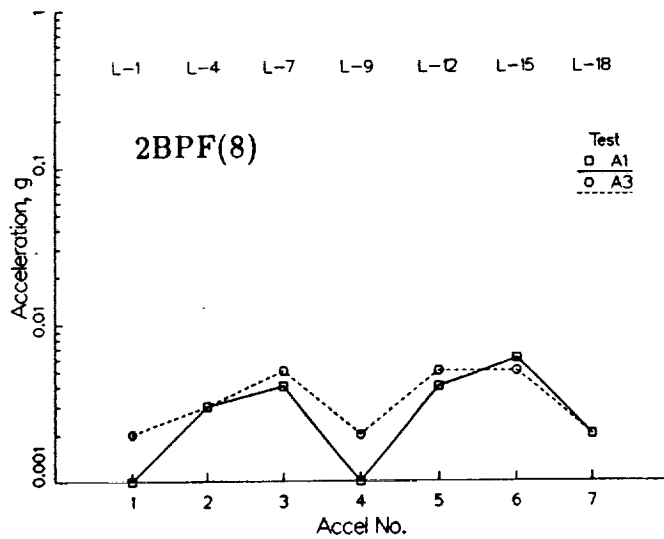
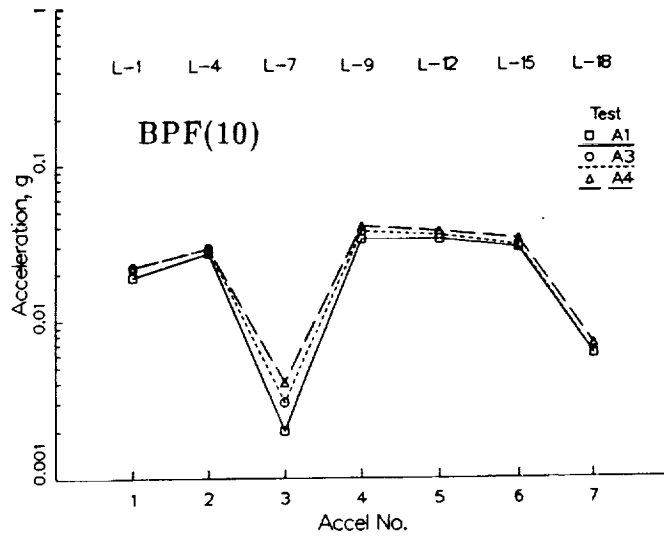
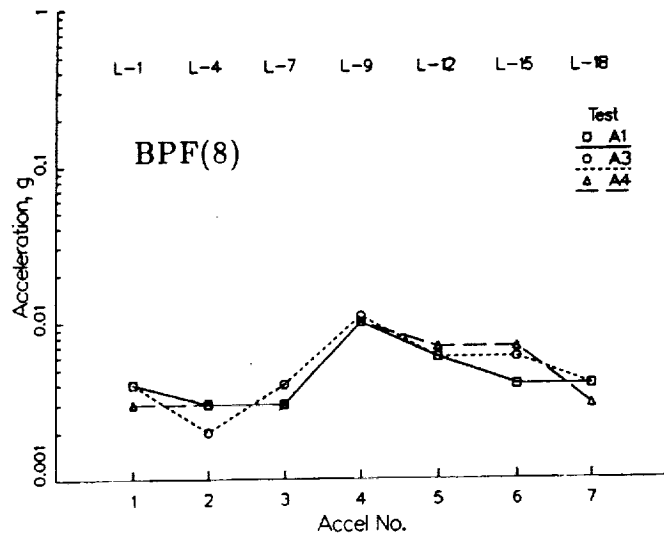


Figure 26. Normalized Frame 758 Accelerometer Levels due to Speaker Excitation, Quiet Cabin Configuration.

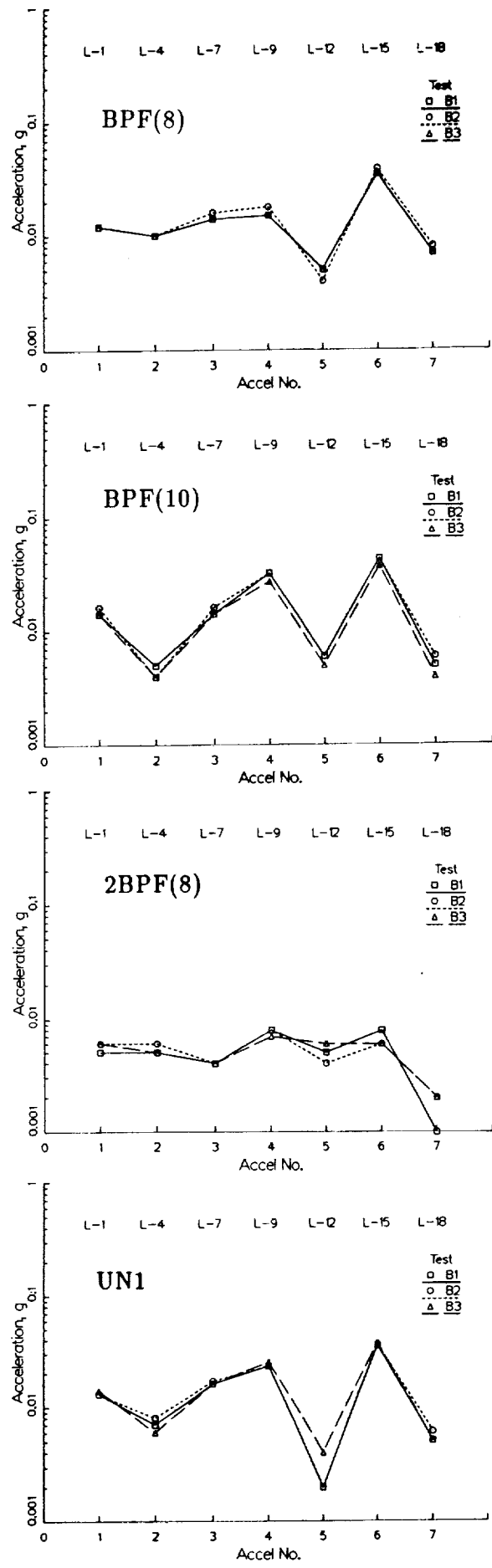


Figure 27. Normalized Frame 758 Accelerometer Levels due to Shaker Excitation, Baseline Configuration.

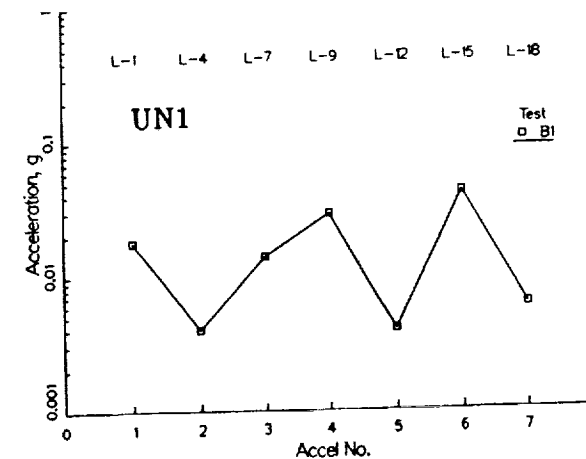
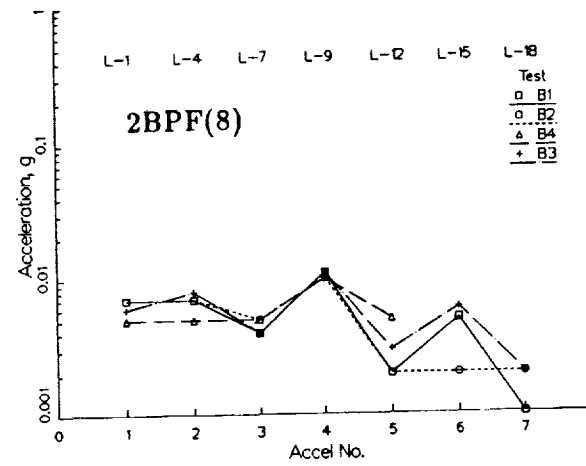
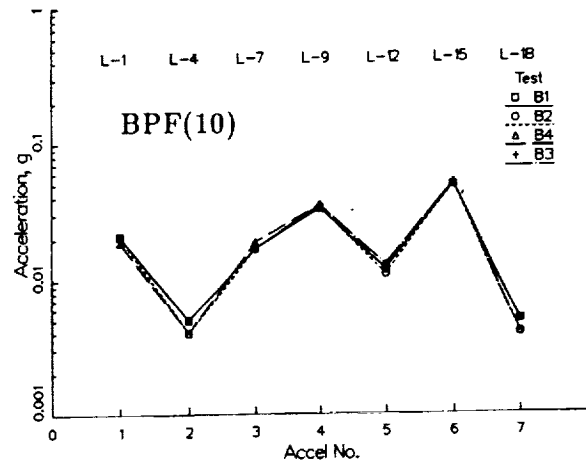
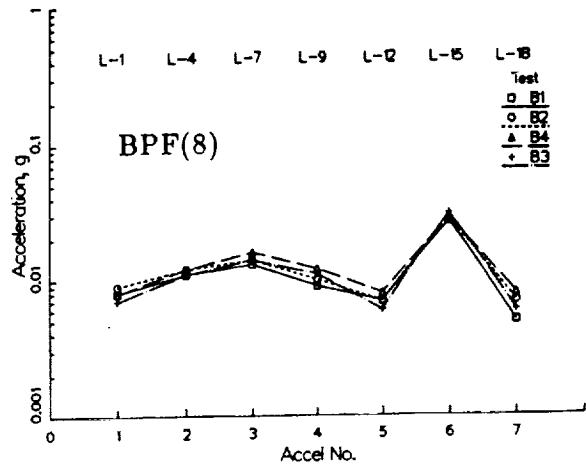


Figure 28. Normalized Frame 758 Accelerometer Levels due to Shaker Excitation, Quiet Cabin Configuration.

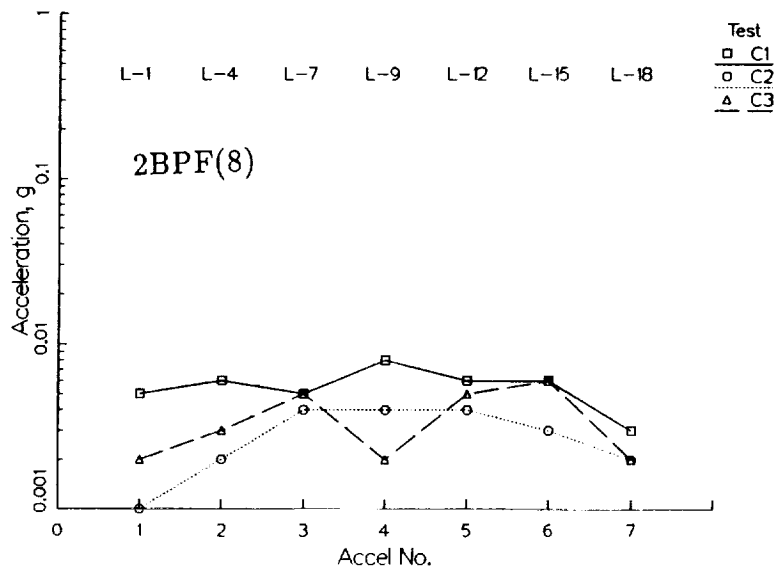
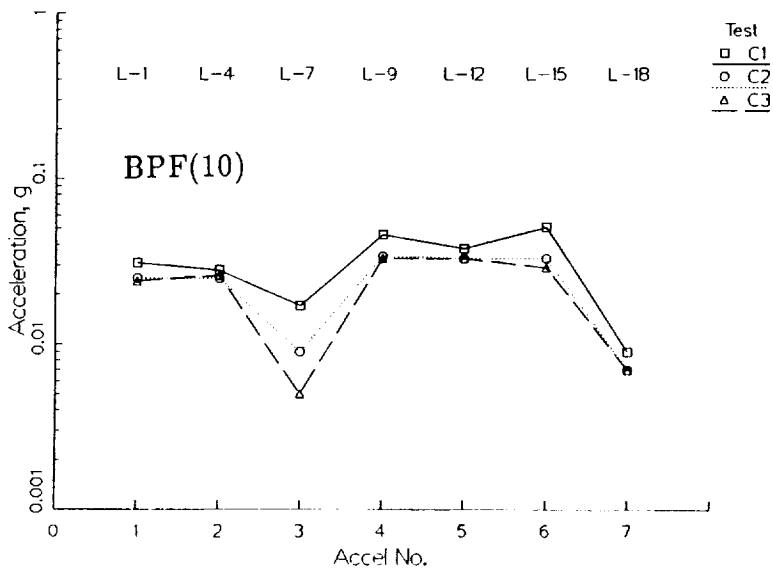
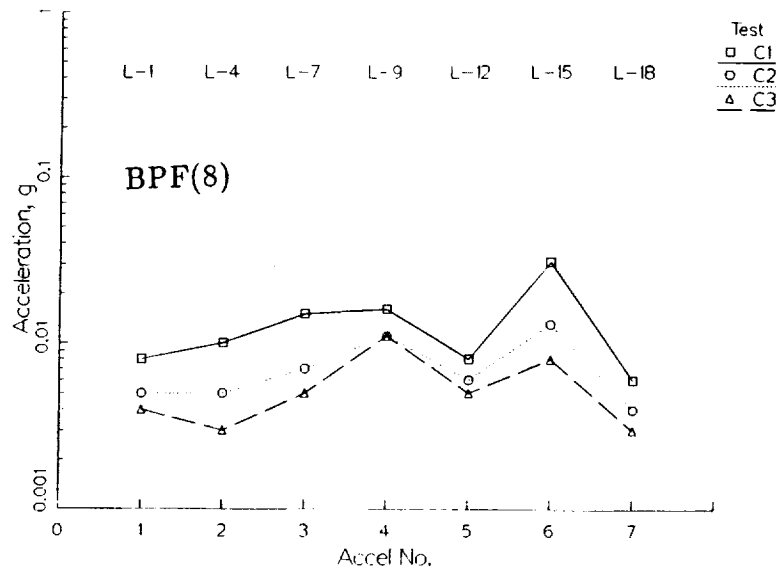


Figure 29. Frame 758 Accelerometer Levels due to Combined Speaker and Shaker Excitation, Quiet Cabin Configuration.

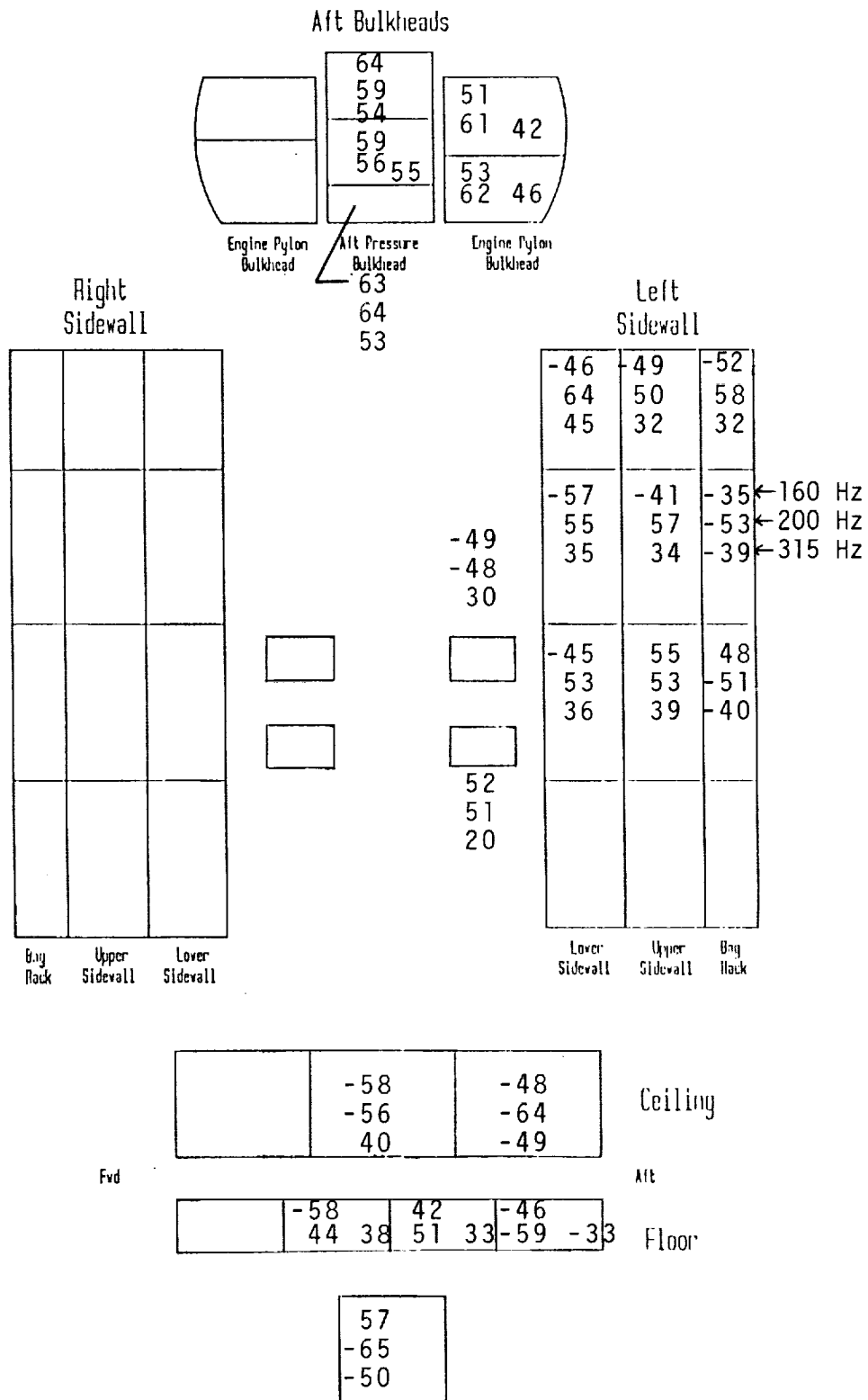


Figure 30. Sound Power Levels due to Speaker Excitation in the 160, 200, and 315 Hz One-Third Octave Bands, Quiet Cabin Configuration.

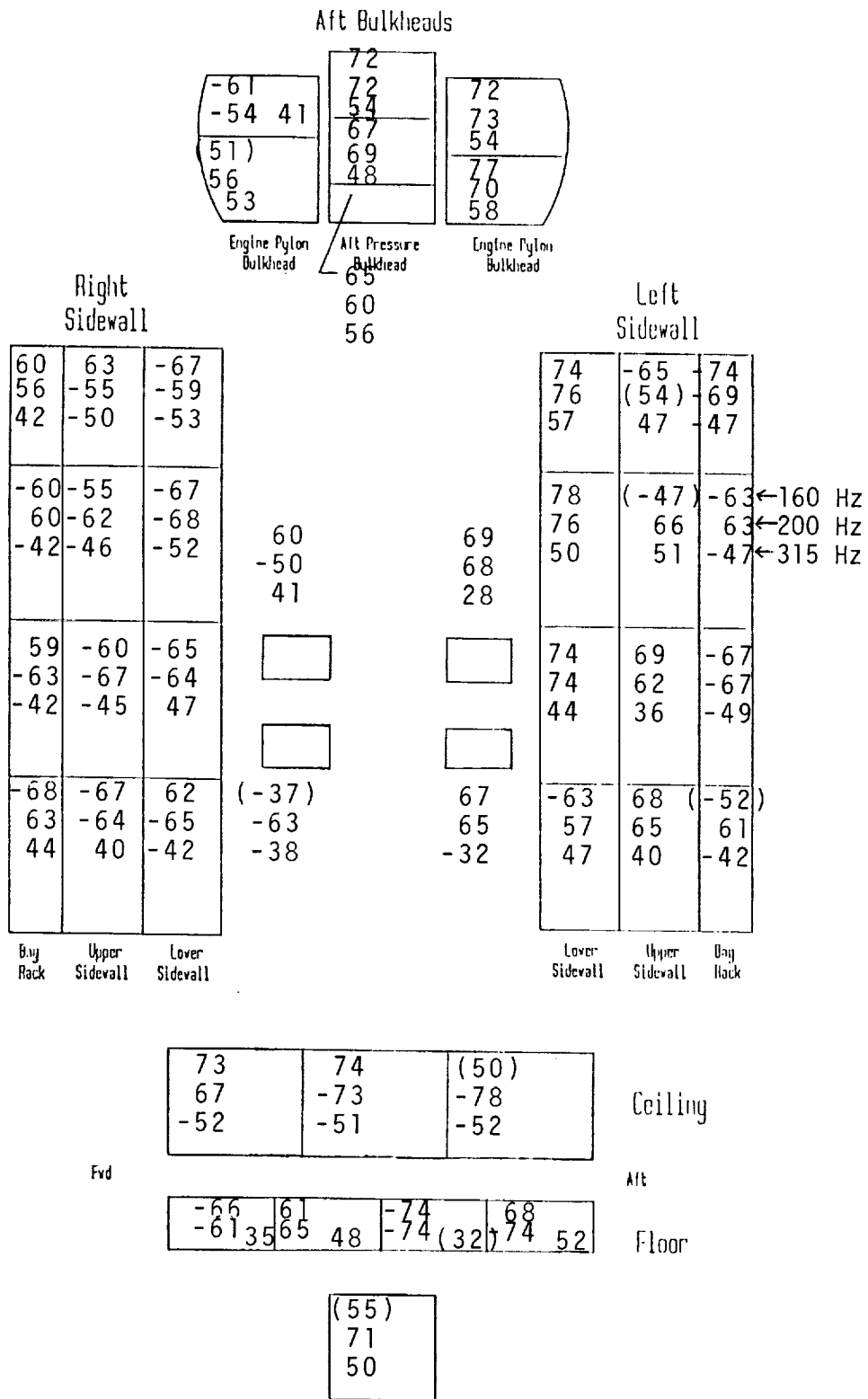


Figure 31. Sound Power Levels due to Shaker Excitation in the 160, 200, and 315 Hz One-Third Octave Bands, Quiet Cabin Configuration.

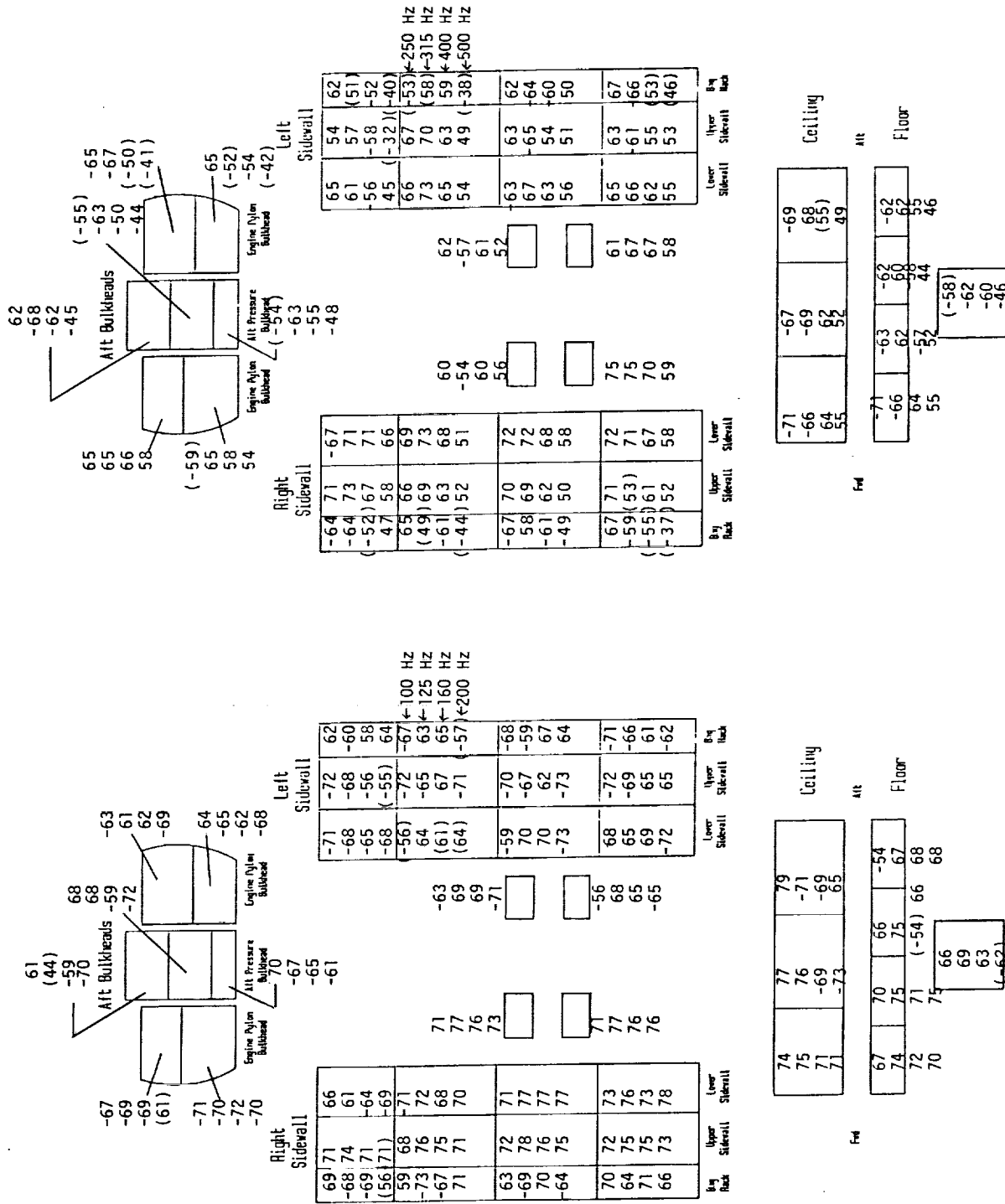


Figure 32. Sound Power Levels due to Speaker Array Excitation in the One-Third Octave Bands from 100-500 Hz, Quiet Cabin Configuration.

4 Comparison of Ground and Flight Test Results

The results of the ground tests reported in the previous section are compared in this section with data collected during the UHB Demonstrator flight tests.

A major concern in the development of effective noise control treatments for UHB aircraft has been the proper identification of major sources of cabin noise and the transmission paths associated with these sources. In Reference [2] the measured Demonstrator noise and vibration data were analyzed to define these sources and paths. The first subsection below analyzes the ground test data and compares conclusions with the flight test results.

In the second subsection, the Quiet Cabin noise levels measured during the ground tests are compared with Demonstrator Quiet Cabin noise levels, after the source input levels are scaled to match the excitation loads occurring in flight. The final subsection addresses the effectiveness of the Quiet Cabin Configuration in reducing cabin noise levels, relative to the Baseline Configuration, as evaluated in the ground and flight tests.

4.1 Identification of Major Transmission Paths

4.1.1 Ground Test Analysis of Transmission Paths

The various blade passage frequency-related tones measured in the cabin are expected to arise from either the acoustic loads on the fuselage (from the dynamic loads on the rotating propellers), or the mechanical forces in the engine (from engine imbalances), or a combination of both. The UN1 tone, related to the engine shaft rotation, can only result from engine forces.

The acoustic excitation could likely be transmitted into the cabin along airborne paths from the propellers through either the cabin sidewall directly into the cabin, or through the aft fuselage into the unpressurized section, then through the pressure bulkhead into the cabin. However, the ground test data show that neither of these paths are significant. Figure 11 shows normalized cabin noise levels for the Quiet Cabin Configuration of around 70 dB, with maximum levels of 80 dB, for the BPF(8) tone. Yet exterior noise levels measured simultaneously on the fuselage surface outside the cabin are 82 to 88 dB and aft fuselage noise levels measured simultaneously behind the pressure bulkhead are 86 to 89 dB (all levels are normalized). For the cabin sidewall and the pressure bulkhead (both of which have noise control treatments), prior ground measurements (Reference [1]) showed transmission losses at the BPF(8) frequency in excess of 30 dB. Thus the interior levels due to airborne propagation through the cabin

sidewall or the pressure bulkhead would be 59 dB or less. Since the measured levels are higher than 59 dB, the airborne paths are not contributing to the cabin noise levels.

This analysis is in agreement with the results of the sound intensity survey which showed that, for speaker excitation, the sidewall is not a major source. The survey also showed that the aft pressure bulkhead and the floor between the lavatories are the major radiating surfaces. Since the airborne transmission through the pressure bulkhead is not significant (as shown above), it can be hypothesized that as the acoustic loads impinge on the aft fuselage and pylon, BPF tones propagate structurally through the aft fuselage to the pressure bulkhead, then radiate into the aft cabin. In support of this hypothesis, analysis of accelerometer data on the aft fuselage and on the pressure bulkhead show relatively high acceleration levels under speaker excitation; the bulkhead BPF(8) acceleration levels are 2 to 14 times higher for speaker excitation than for shaker excitation, for the same resulting maximum noise levels in the cabin.

The sound intensity survey for the shaker excitation indicated that for all tones (including UN1), the major radiating surfaces were the left pylon bulkhead, the pressure bulkhead, and the left sidewall. If the BPF tones in the cabin are propagated structurally, what is the proportion due to acoustic loads impinging on the fuselage versus engine mechanical forces? In Section 3 the interior noise levels and frame acceleration levels due to combined speaker and shaker excitation were reviewed. From both the noise and acceleration data it was observed that shaker excitation dominated the cabin noise levels for Test C1 (with the highest shaker input), and speaker excitation dominated the cabin noise levels for Test C3 (with the lowest shaker input).

The pylon acceleration levels measured on the Demonstrator were reviewed and compared with the acceleration levels used in the ground tests. This analysis showed that when the speaker and shaker excitations are scaled to simulate the full loads occurring on the actual aircraft during flight (see discussion below), the Test C3 relative excitations are in closest agreement with flight conditions. On this basis, it can be concluded that the airborne excitation of the fuselage propagating along a structureborne path is the major contributor to cabin noise levels for BPF tones, followed by the structureborne propagation of engine mechanical forces.

Although the airborne transmission path through the cabin sidewall is not a significant path for BPF tones, it is reasonable to expect that the exterior turbulent boundary layer noise is transmitted into the cabin along this path, to form the broadband, background portion of the interior noise spectrum.

4.1.2 Comparison With Flight Test Analysis

Several approaches to identifying major transmission paths on the Demonstrator were used in Reference [2], including partial coherence analyses of measured noise and vibration data and analysis of measured in-flight sound intensity data. The conclusions reached in that report are as follows:

- “the cabin sidewall path is not a propeller noise path but is the likely path of the broadband noise component,
- “the aft section path does not appear to be a transmission path for the propeller noise and
- “the tones found in the interior noise spectra are the result of structureborne transmission through the pylon and the fuselage. The transmitted energy is caused by a combination of acoustic loads from the propeller blades impinging on the pylon, and mechanical forces within the engine propagating through the pylon.”

It is clear that these conclusions are nearly identical to those developed above, except that analysis of the Demonstrator data did not provide a determination of the relative importance of the two structureborne paths. This is because the paths were coincident, and the acoustic loads and mechanical forces were operating simultaneously. For the ground tests, it was possible to excite the structure individually with (simulated) acoustic loads and mechanical forces, as well as with varying combinations of the two, and thereby study in more detail their relative strengths. In this regard the ground tests allow more flexibility in fully identifying transmission paths.

It should be noted, however, that the ability to diagnose the relative strengths of two separate paths from ground test data is dependent on knowledge of the relative strengths of the excitation forces. In the analysis above, the acoustic and vibratory loads measured on the Demonstrator were used to scale the speaker and shaker input levels for the ground tests. If these data were unavailable, engineering estimates of these excitation levels would be needed, and the accuracy of the resulting transmission path determination would be critically tied to the accuracy of these estimates of input forces.

4.2 Cabin Noise Levels

Based on the transmission path analysis described above, interior noise levels measured at selected seat locations in the test fuselage due to individual speaker and shaker

excitation were adjusted, after scaling the input excitation levels to match the corresponding levels measured in flight.

Since the cabin noise levels for BPF tones resulting from speaker excitation were found to be structurally propagated, scaling of the speaker input was based on the acceleration levels measured at the aft fuselage accelerometer in the (simulated) propeller plane. Note that scaling the speaker input based on aft fuselage exterior noise levels resulted in unrealistically high scaled interior noise levels.

For the shaker excitation, scaling was based on acceleration levels measured at the forward engine mount, at the intersection of the pylon and the fuselage.

The scaled interior noise levels are shown in Figure 33, for the BPF(8), 2BPF(8), and UN1 tones. The figure compares the ground test results with the corresponding tone levels measured on the Demonstrator, for the ten seat locations where both ground and flight data are available. For the two BPF tones, there is good agreement between the Demonstrator levels and the ground test levels due to speaker excitation. As expected from the discussion above, agreement with shaker-generated levels is poor for these tones. For the UN1 tone, Demonstrator and ground test levels (shaker excitation) are in good agreement.

For these comparisons, "good agreement" does not mean that the noise level at every seat is the same for the ground and Demonstrator data. Rather, the maximum levels among all the seats are comparable between the ground and flight test measurements, and the average or typical levels are also comparable. The differences shown in Figure 33 between ground and flight test noise levels for individual seats may be due to differences in the phase distribution of the incident acoustic field between the speaker excitation on the ground and the UHB engine excitation in flight; the phase distribution will influence the coupling between the acoustic field and the structural response, thereby affecting the cabin noise levels. Although the acoustic loads distribution on the ground simulated the actual loads in flight reasonably well (see Figure 3), no attempt was made to simulate the actual phase distribution in the ground tests.

Thus far in this section all data have been presented for a simulated rotor speed of 1260 rpm. Figure 34 compares ground test noise levels for BPF(8) under speaker excitation with Demonstrator noise levels, measured over a range of rotor speeds. The cabin noise levels shown are the maximum noise levels in cabin rows 4 and 6. The agreement is good for the row 4 data, but the row 6 data are in poor agreement. This discrepancy reflects lower maximum BPF(8) levels on the Demonstrator in row 6 than in row 4, while the reverse occurs in the ground tests.

To compare the broadband noise in the cabin due to speaker array excitation with broadband levels measured in flight, the one-third octave band levels measured at the speaker array reference microphones (see Figure 4) were scaled to the boundary layer

noise levels measured on the Demonstrator outside the last cabin seat row. Figure 35 shows the exterior spectra measured during the ground tests at the two reference microphones, as well as the resulting interior spectra at an aft cabin seat location. Scaled one-third octave band levels at this cabin location are compared to measured interior levels on the Demonstrator in Table 2 below. (Note that the 125, 160, and 200 Hz levels are omitted since the Demonstrator measurements contain various engine and BPF tones in these one-third octave bands). The table shows reasonably good agreement (within 3 dB) for the one-third octave bands at 250 Hz and above, but poor agreement at 100 Hz.

TABLE 2. COMPARISON OF BROADBAND CABIN NOISE LEVELS MEASURED DURING GROUND AND DEMONSTRATOR FLIGHT TESTS

<u>1/3 Octave Band, Hz</u>	<u>Broadband Sound Pressure Level, dB</u>	
	<u>Ground Data*</u>	<u>Demo Data</u>
100 Hz	88	80
250 Hz	79	77
315 Hz	79	76
400 Hz	78	76
500 Hz	73	70

*Levels scaled from ground tests, based on levels at the speaker array reference microphones.

4.3 Evaluation of Treatment Effectiveness

Figures 10 and 11 show Baseline and Quiet Cabin Configuration noise levels, respectively, measured during the ground tests for speaker excitation. Corresponding measured levels for shaker excitation are shown in Figures 15 and 16. From these figures the change in noise levels resulting from installation of several treatments can be seen: for the BPF(8), BPF(10), and 2BPF(8) tones the ground test data for speaker excitation in Figures 10 and 11 should be used since it was found that the levels in the Demonstrator cabin for these tones were caused by propeller-generated acoustic loads, while the ground test data for shaker excitation in Figures 15 and 16 should be used for the engine-generated UN1 tone.

On these figures noise levels are shown for 17 seat locations; corresponding Demonstrator data for the same two configurations are available only for four of the seats in row 4 (corresponding to seats 2 – 5 in the ground tests) and for the six seats in row 6 (corresponding to seats 12 – 17 in the ground tests). For these ten aft cabin locations, Table 3 below shows the differences in the maximum noise levels of each tone, measured for the Baseline and the Quiet Cabin Configurations. The table also lists differences in the broadband noise levels measured for the two configurations, in terms of A-weighted overall levels and the level over two frequency ranges.

The noise level differences in Table 3 can be considered a measure of the effectiveness of the treatments installed on the aircraft between the two configurations. Note that in Reference [2], treatment effectiveness data are provided in terms of differences in maximum levels for the row 6 seats only. Since BPF noise levels measured on the Demonstrator in row 4 were higher than in row 6, the comparison of ground and flight data in Table 2 uses levels measured in both row 4 and row 6.

The table shows reasonably good agreement between the ground test results and the flight test results, for both the tone and broadband components of the spectrum. In contrast to the transmission path comparisons discussed above, these comparisons are independent of absolute levels, and therefore do not rely on knowledge of source excitation levels (either measured or estimated). These results indicate that ground testing of candidate noise control treatments can provide an accurate assessment of the effectiveness of these treatments during actual flight conditions.

TABLE 3. NOISE LEVEL REDUCTION BETWEEN BASELINE
AND QUIET CABIN CONFIGURATIONS

A. TONE COMPONENTS

<u>Tone</u>	<u>Reduction in Maximum Level, dB</u>	
	<u>Ground Data</u>	<u>Demo Data</u>
BPF(8)	-1	0
BPF(10)	6	*
2BPF(8)	7	5
UN1	3	2

B. BROADBAND COMPONENT

<u>Frequency Range</u>	<u>Reduction in Spectral Level, dB</u>	
	<u>Ground Data</u>	<u>Demo Data</u>
A-Weighted OA	5	5
200-350 Hz	8	7
350-500 Hz	7	8

*BPF(10) data are unavailable.

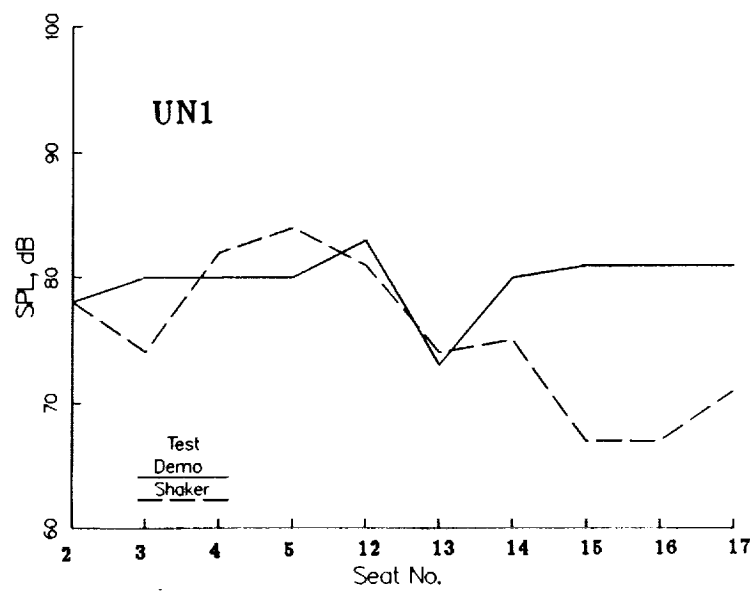
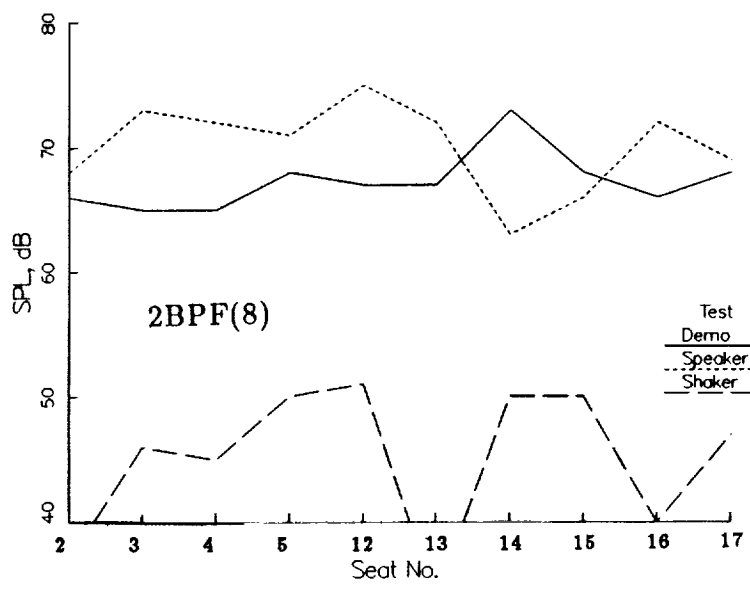
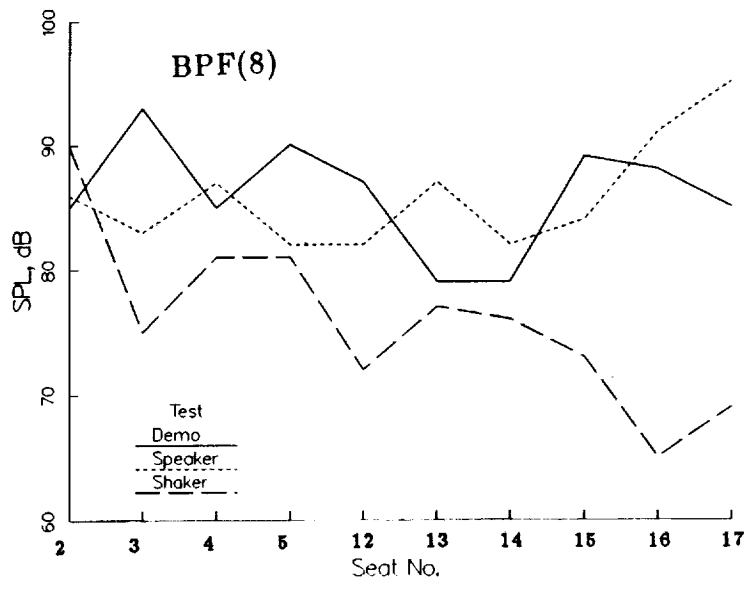


Figure 33. Comparison of Cabin Noise Levels Scaled from Ground Test Measurements with Flight Test Data, Quiet Cabin Configuration.

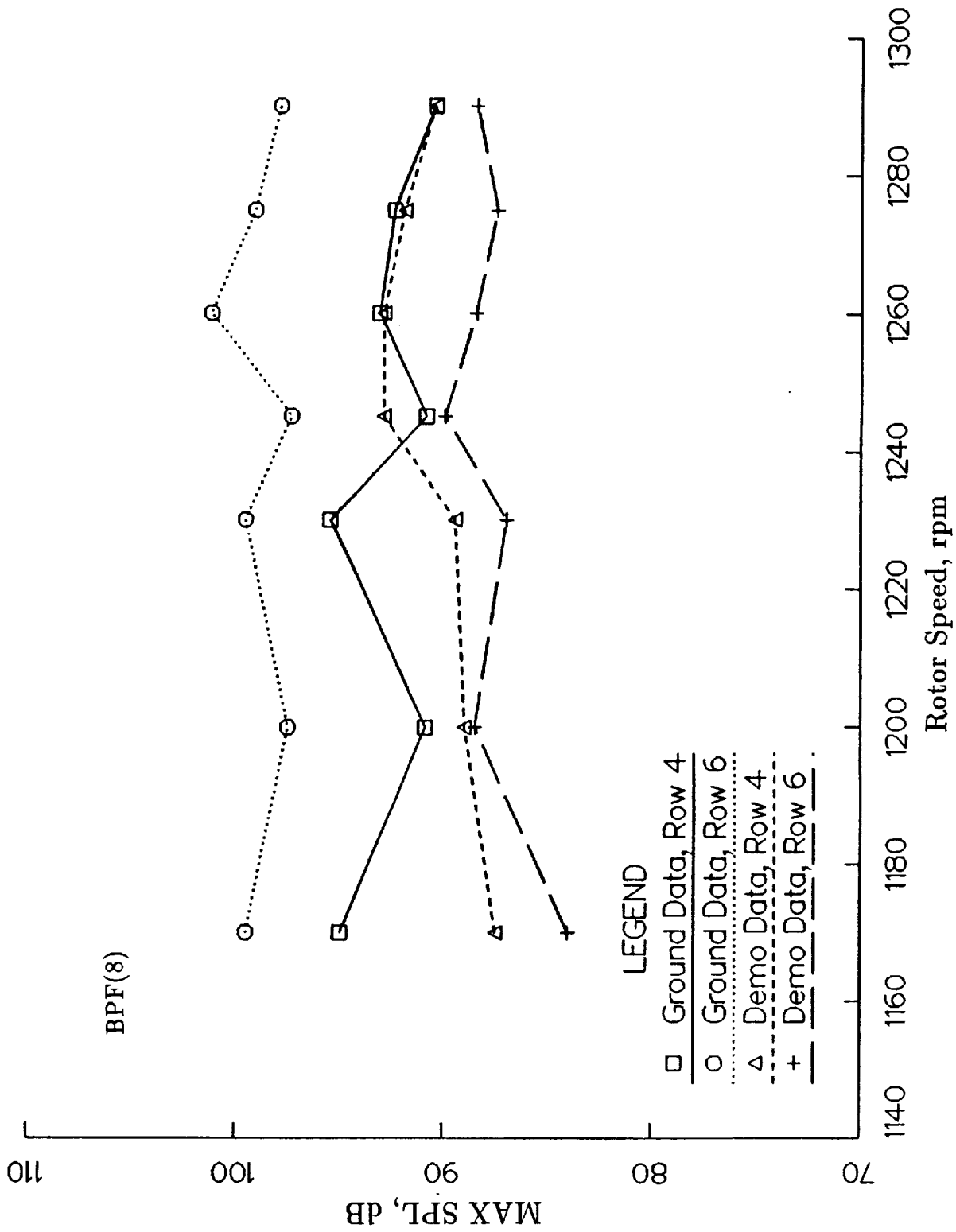


Figure 34. Comparison of Maximum Cabin Noise Levels Measured During Demonstrator and Ground Tests for Varying Rotor Speed, Quiet Cabin Configuration.

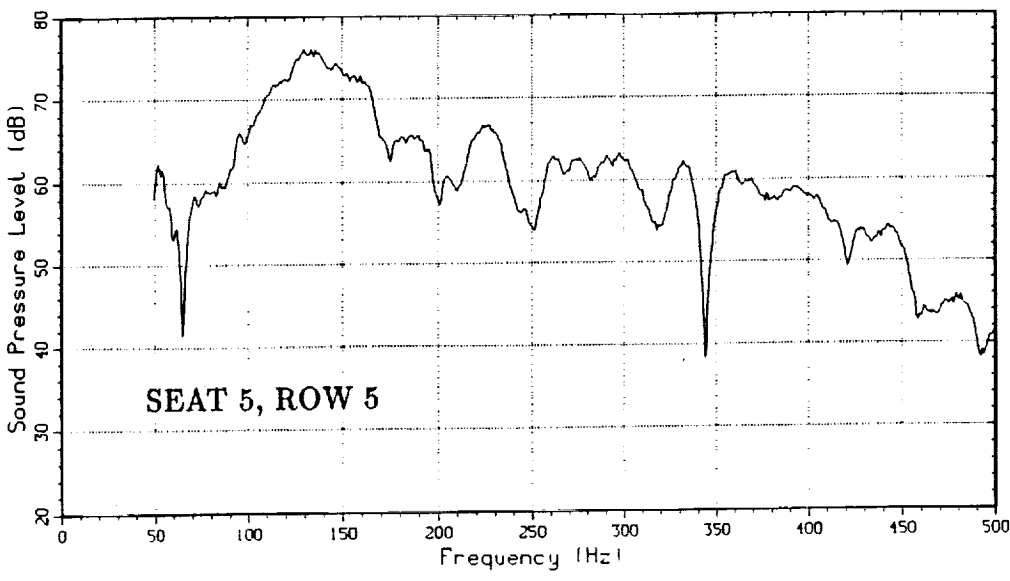
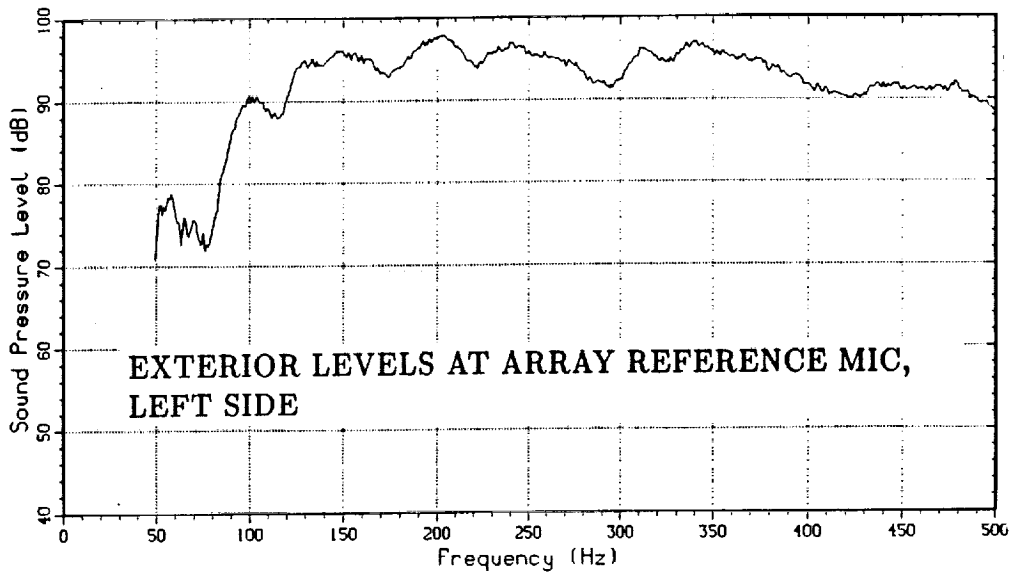
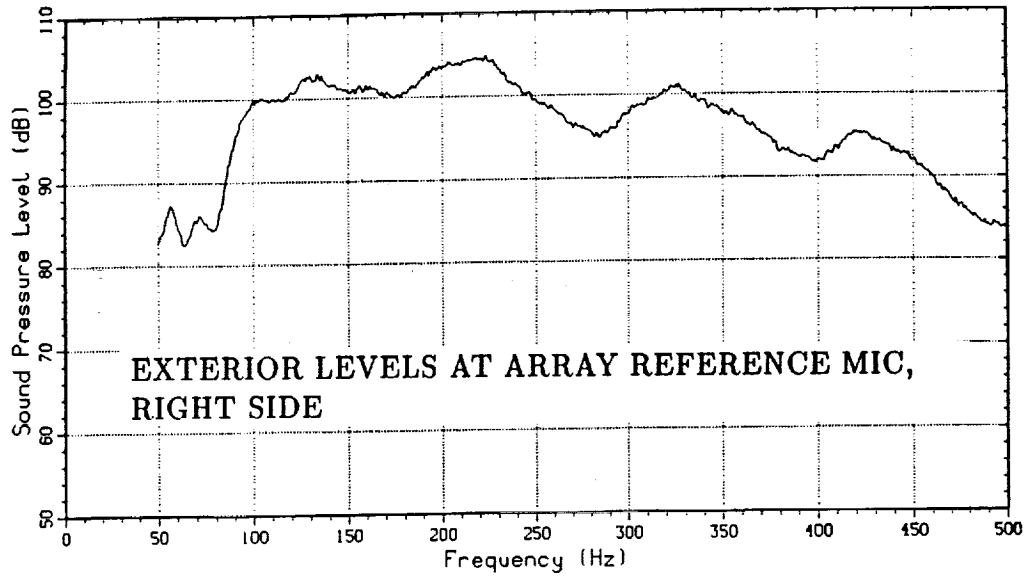


Figure 35. Exterior and Interior Spectra due to Speaker Array Excitation Measured During Ground Tests, Quiet Cabin Configuration.

5 Summary and Conclusions

A series of ground tests were conducted in FARF to measure noise and vibration levels under simulated advanced turboprop excitation, for two fuselage configurations representing different noise control treatment packages. The measured data were compared with UHB Demonstrator flight test data collected under comparable treatment configurations. The major purpose of these tests and comparisons was to study ground test and analysis techniques for assessing noise control treatment effectiveness for UHB aircraft. In addition, the effect of variations in test conditions on the ground measurement results was to be evaluated.

For the ground tests, various treatments were installed on the DC-9 fuselage test section to represent the Baseline and Quiet Cabin Configurations on the Demonstrator. Three lab sources were used to simulate the acoustic and vibratory excitation of advanced turboprop aircraft: a single speaker for the acoustic loads on the fuselage from propeller tones, a shaker for engine-generated structureborne tones, and an array of speakers for broadband turbulent boundary layer noise. For these excitations, singly and in combination and for various input levels, cabin noise levels and frame acceleration levels were measured at selected locations. A sound intensity survey was also conducted to identify the major radiating surfaces for each type of excitation.

Results of the ground tests are as follows:

- For all excitations, the fuselage responds linearly to input loads. That is, as the speaker input levels change by 6 dB, the resulting cabin noise levels and frame acceleration levels change by 6 dB. As the shaker input forces vary by a factor of 2, the resulting cabin noise levels and frame acceleration levels vary by 6 dB. As the speaker array input levels change by 6 dB, the resulting cabin noise levels change by 6 dB.
- There are small variations in cabin noise levels for individual propeller tones under speaker or shaker excitation as the blade passage frequency varies with engine speed over the typical operating range.
- Differences in level of pressurization affect cabin noise levels, particularly for shaker excitation. For speaker and speaker array excitation, the biggest variation occurs between pressurized and unpressurized conditions.
- Broadband excitation and tonal excitation result in comparable cabin noise levels on average, but the spatial distribution is less uniform under tonal excitation for speaker and shaker inputs.

- Combined speaker and shaker excitation result in cabin noise levels and frame acceleration levels comparable to the sum of the levels from the individual excitations.
- The relative phase between speaker and shaker inputs for combined excitation does not significantly affect resulting cabin noise levels.
- The differences in cabin noise levels between the Baseline and Quiet Cabin Configurations for BPF tones are greater under shaker excitation than speaker excitation. The differences in acceleration levels between the two configurations are negligible for both excitations.
- The sound intensity survey showed that for speaker excitation the major radiating surfaces for BPF tones include the aft pressure bulkhead (all tones) plus the left pylon bulkhead and aft sidewall (BPF(10) tone). For shaker excitation the major radiating surfaces for the UN1 tone are the aft bulkheads and left sidewall. For speaker array excitation the sidewalls are the major radiating surfaces.

Analysis of the ground test results, scaled to measured Demonstrator acoustic and vibratory loads, revealed that the BPF tones in the cabin arise from propeller-induced acoustic loads impinging on the aft fuselage and then propagating structurally through the fuselage. Structureborne propagation of engine-generated tones was found to be a minor source of cabin tones.

Previous analyses of Demonstrator data showed similar conclusions, indicating that ground tests can provide information on transmission paths that is comparable to that derived from flight tests. Indeed, if the relative strengths of suspected sources or paths are known, the ground tests can provide more detailed information than the flight tests can provide.

Comparison of scaled ground test data with Demonstrator data also showed that cabin noise levels measured on the ground are in good agreement with levels measured in flight for the BPF and UN1 tones. The exact pattern of interior levels by seat measured on the Demonstrator was not duplicated in the ground measurements, but the maximum levels and average levels among the measurement locations were in close agreement between the ground and flight tests.

For the broadband component of the cabin noise spectrum, ground test results are in good agreement with levels measured in flight, except in the low frequency region.

Finally, differences in cabin noise levels due to fuselage configuration changes were determined to assess treatment effectiveness. Comparison of these differences as determined from the ground tests and the flight tests again showed close agreement.

The measurements and analyses in this report demonstrate that carefully planned and executed ground tests can provide extremely useful information on transmission paths, treatment effectiveness, and absolute noise levels, particularly for the tones generated by advanced turboprop engines and propellers. When flight tests are impractical or limited, ground tests can furnish valuable insight in the design of effective cabin noise control treatments. To ensure the accuracy of ground test results, the test article and noise and vibration sources should simulate reality as closely as possible.

6 References

- [1] Simpson, M. A., et. al., "Interior Noise Control Ground Test Studies for Advanced Turboprop Aircraft Applications," NASA Contractor Report 181819, April 1989.
- [2] Simpson, M. A., et. al., "UHB Demonstrator Interior Noise Control Flight Tests and Analysis," NASA Contractor Report 181897, October 1989.
- [3] Simpson, M. A., et. al., "Fuselage Shell and Cavity Response Measurements on a DC-9 Test Section," NASA Contractor Report 187557, August 1991.



Report Documentation Page

1. Report No. NASA CR-187558	2. Government Accession No.	3. Recipient's Catalog No.	
4. Title and Subtitle Analysis of Interior Noise Ground and Flight Test Data for Advanced Turboprop Aircraft Applications		5. Report Date August 1991	6. Performing Organization Code
		8. Performing Organization Report No.	
7. Author(s) M. A. Simpson and B. N. Tran		10. Work Unit No. 535-03-11-03	
		11. Contract or Grant No. NAS1-18037	
9. Performing Organization Name and Address Douglas Aircraft Company McDonnell Douglas Corporation 3855 Lakewood Blvd. Long Beach, CA 90846		13. Type of Report and Period Covered Contractor Report	
		14. Sponsoring Agency Code	
12. Sponsoring Agency Name and Address National Aeronautics and Space Administration Langley Research Center Hampton, VA 23665-5225		15. Supplementary Notes Langley Technical Monitor: Kevin P. Shepherd Final Report - Task 8	
16. Abstract <p>This report describes interior noise ground tests conducted on a DC-9 aircraft test section. The objectives of this work were to study ground test and analysis techniques for evaluating the effectiveness of interior noise control treatments for advanced turboprop aircraft, and to study the sensitivity of the ground test results to changes in various test conditions.</p> <p>To meet these objectives, noise and vibration measurements were conducted on the DC-9 test section under simulated advanced turboprop excitation, for two interior noise control treatment configurations. Selected test conditions were parametrically varied during the test to examine sensitivity effects. These ground measurement results were compared with measurement results obtained during earlier UHB Demonstrator flight tests with comparable interior treatment configurations. The Demonstrator is an MD-80 test aircraft with the left JT8D engine replaced with a prototype Ultra High Bypass (UHB) advanced turboprop engine.</p>			
17. Key Words (Suggested by Author(s)) Acoustics Advanced Turboprop Aircraft Aircraft Noise Flight and Ground Tests Interior Noise Control		18. Distribution Statement Unclassified - Unlimited Subject Category - 71	
19. Security Classif. (of this report) Unclassified	20. Security Classif. (of this page) Unclassified	21. No. of pages 66	22. Price

